

# Determining personality typology through psycho physiological inference from EEG and EDA biosignals

Author: Dumitru GRIGORE, PhD

## Abstract

Research described in present study approaches EEG biosignals physiology and power spectral distribution, respectively EDA phenomenology, highlighting electrodermal potential technique in alternating current. The experiment structure is based on a design adequate to specific purpose of the topic, i.e. recourse to two distinct techniques pertaining to quoted biosignals, in view of obtaining the same type electrical behavior, expressed as personality typology. We determined the projective functions using, for EEG, power spectral density as measured by the NeuroSky MindSet headset; whereas for EDA, we considered the skin alternating current potential levels, basal type (SPL) and response type (SPR), acquired through MindMi™ assessment system, patented by author of present research, in 2013.

**Key words:** bio-signals, electrodermal response, BCI systems, biofeedback

## 1.General

Research applied in neural engineering, cognitive engineering and cognitive sciences is of paramount importance worldwide. Today's brain research implies advanced techniques and technologies, among which, notably, magnetic resonance imaging, which supplies valuable information on the brain regions as activated by stimuli. Such images, reproduced by evocation, ascertain and certify the concept *pattern recognition*, which comes particularly useful in charting procedures. Electroencephalography techniques (EEG) are also used for brain charting, at a lower resolution though. All of such aspects of experimental research become coherent and meaningful under the auspices of the new concept *neural engineering*, implementable in neurotechnology. *Neural engineering* is revealed through all of the interdisciplinary criteria generically attributed to techno psychology, based on research of the relationship amongst neurons, neural networks and the nerve system functions; also, as based on quantifiable models, aiming to develop and implement measuring and control techniques, of sleepy devices.

Neural engineering is directed towards human-machine interaction, (HCI – Human Computer Interaction); by further specialization, such engineering may go beyond usage in psychology, thus opening prospects for robotics, or for the virtual and informatics technologies, naturally sharing the

method with cognitive engineering, yet distinctly apart, in terms of implementation of specific hard.

Brain-computer interfacing would be one type of direct communication between brain and external device, already proven useful as improving, recouping and substituting cognitive or human sensory-motor functions.

Electrodermal activity (EDA), is a widely used phenomenology in measuring systems of, psychophysical aspects, applied in the case of the well known polygraph (lie detector), and basic for a number of measuring devices used these 30 years to identify series of major psychophysical data.

However, such research does not cover all of the complex aspects required for drawing – by inference from physiological data – a good enough mix of cognitive aspects, to safely involve in command and remote control of movement in technical systems.

Research covered by present study cannot be covered within one single discipline. Thus, our topic needs to develop based on a robustly reasoned multidisciplinary approach, since so many applications require electronics and electro-mechanical engineering, e.g. the physics of signals to start with, and the mathematics of processing thereof, up to the psychophysical phenomenology expressed as an advanced mix of patterns.

Such approach implies studying interface phenomena, enabling engineering to implement input neurosignals acquired by specific procedures, corresponding to specific psychophysical aspects.

By present research, a global vision is depleted, of ways to identify psychophysical factors able to grow into patterns of bio-signals taken over by means of measuring technologies, through a direct, noninvasive, rapid and quite accurate method. For such purpose, on the one hand a measuring system approved for EEG bio-signals was used; whereas on the other, a *skin phase neural stimulation* procedure in an original concept was used, as well as equipment and a method able to identify a psychological profile quite fast, as patented by present research author, [Grigore, 2013].

Present study mainly targets a determination of the correlation among biosignals patterns, distinct in terms of physiology and acquired through specific equipments. Present research extends an original technical solution, to add up to the current field research.

The research-proper implies running multiple, exemplifying measurements, of specific patterns of various physiologies' biosignals, by making use an

adequate type design, processing experimental data and elaborating the statistical study on the correlation of the two biosignals categories, carrying out in own patterns same common action structures, by means of which it is possible to set up a redundant *experience basis*.

Veracity validation, of results yielded by the original approach of EDA phenomenology in present research, was through assessment by direct measurement of a number of subjects; such subjects were measured simultaneously, at forehead level, for EDA type signals, respectively EEG type signals. Such signals were later converted into a set of values

## 2. EEG biosignals

### 2.1 The physiology of EEG biosignals

Basic components of CNS are the nerve cells (neurons) and glial cells, in-between the neurons, each nerve cell consisting of an axon, dendrites and cell body, as indicated in Fig.1, a. Nerve cells transmit information through the body as electrical impulses. The axon acts as a pathway conductive of the electrical impulse, whereas the dendrites connected either with other axons, or with other dendrites, distribute the impulse towards other nerve cells [Sanei & Chambers, 2008].

In the nerve cell various electrical impulses may occur. When an action potential (AP) stimulates excitatory synapses, an excitatory postsynaptic potential (EPSP) is produced. An inhibitory postsynaptic potential (IPSP), which illustrates hyperpolarization, is produced when an inhibitory synapse is stimulated by an AP [Sanei & Chambers, 2008; Fox, 2009; Lopes, 2010]. EPSP or IPSP are generated in ulterior nerve cells, by the active postsynaptic current, as indicated in Fig.1, b. After an EPSP or IPSP occurs, a potential is produced along the cell nerve, due to the difference of the percentage of cations (positive load ions) and anions (negative load ions) between the nerve cell exterior and interior. Primary transmembrane currents generated extracellular currents which are responsible for the generation of field potentials [Sanei & Chambers, 2008; Lopes, 2010].

The nerve cells transfer information as AP. An AP is generated by the ions exchange which diffuse through the neuron membranes, thus creating a temporary change of the membranes potential. The ions exchange is caused by a PPSE, which must go beyond a threshold potential for an AP to be initiated. In order for a threshold to be surpassed, a higher number of presynaptic neurons must similarly produce a PPSE [Zinke-Allmang, 2009], as indicated in Fig.2, a.

expressing, for EDA, electrodermal potential levels (SPL), respectively by electrodermal response potentials (SPR); whereas for EEG, *power spectral density*, for the corresponding brain frequency bandwidths.

Thus, present experimental study is run through two distinct techniques based on bio-signals, in order to obtain, by inference, in variables corresponding to each distinct technique, the same type behavior, expressed as electrical signals.

During the ions exchange, the membranes potential depolarizes fast, rising in positive polarity and creating a peak. The membranes potential repolarizes in order to rebalance, back to the original membranes potential, known as rest membranes potential [Sanei & Chambers, 2008; Fox, 2009; Zinke-Allmang, 2009].

Fig.2, b indicates an AP peak produced when a neuron is stimulated. The predominant ions implied in the AP peak are Na<sup>+</sup> and K<sup>+</sup>. When a neuron is stimulated, a rapid repolarizing occurs, whereat the Na<sup>+</sup> channels with voltaic gate open and permit Na<sup>+</sup> to diffuse into the nerve cell membranes, increasing potential thereof. If such potential touches at the -55 mV threshold, then a higher number of Na<sup>+</sup> voltaic gate channels open and permit an increased quantity of Na<sup>+</sup> to diffuse, causing membranes potential to increase to +30 mV [Sanei & Chambers, 2008]. Before touching at the peak, the Na<sup>+</sup> with voltaic gate channels become inactive, and Na<sup>+</sup> stops diffusing. The K<sup>+</sup> with voltaic gate channels open and K<sup>+</sup> start diffusing outside of the cell membranes, thus lowering the membranes potential. Such process is known as repolarizing. Channels with Na<sup>+</sup> voltaic gate become active again and Na<sup>+</sup> start diffusing anew, up to balance (rest membrane potential) point [Sanei & Chambers, 2008].

During the balancing process, re-polarization goes beyond the rest potential (see Fig. 2, b). Such phenomenon is known as hyperpolarization. Hyperpolarization is a safety action which prevents the neuron from receiving other stimuli, potentially causing further AP in the opposite direction [Sanei & Chambers, 2008]. Post hyperpolarization, membranes potential returns to (-70 mV) rest level. The whole process, recouping time included, before another AP is generated, takes 8ms [Zinke-Allmang, 2009].

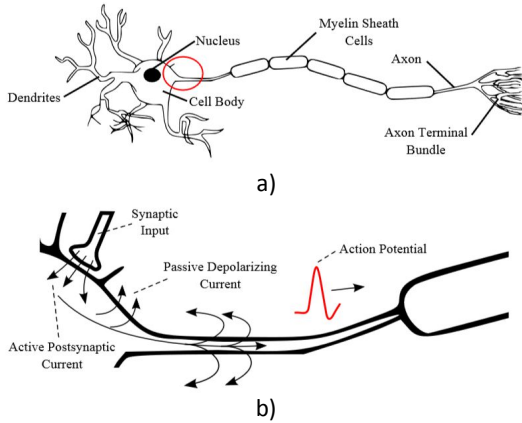


Fig. 1. NCS cells: (a) anatomy and (b) electrical impulse generation [Sanei & Chambers, 2008].

The brain neurons produce AP, which contributes to the neural generation activity recorded by EEG. There are  $10^{10}$  up to  $10^{11}$  neurons in the brain and the sum up of activity thereof is responsible for the production of neural activity [Nunez & Srinivasan, 2009]. While tens of thousands pyramidal neurons are being excited, a current flow is generated, which, in turn, generates electrical dipoles between neuron body and dendrites.

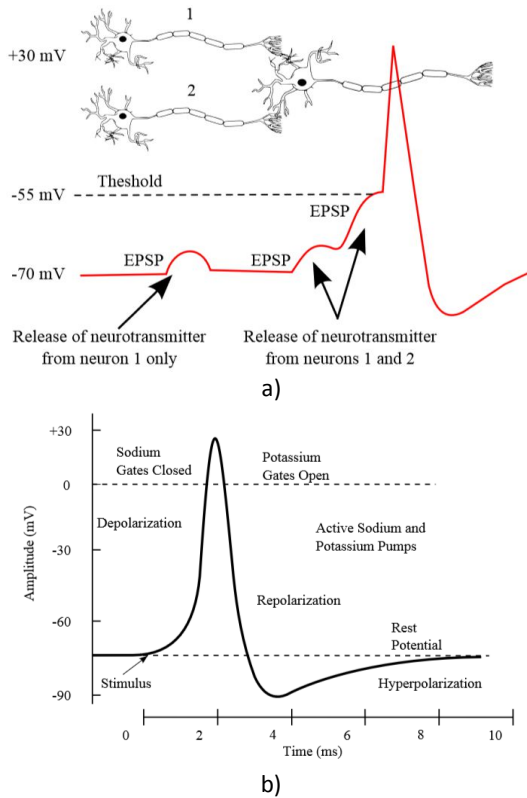


Fig. 2. Action potentials: (a) threshold limit and (b) ion exchange during generation [Sanei & Chambers, 2008; Fox, 2009]

EEG is a technique used for measuring electrical dipole between 2 distinct locations in the brain, such dipole being generated by the brain cortex [Teplan, 2002] (see Fig. 3). An EEG signal, measured at scalp level, is generated by the inhibitory postsynaptic potentials (IPSP) and by the excitatory postsynaptic potentials (EPSP) [Kandel, Schwartz & Jessell, 1991].

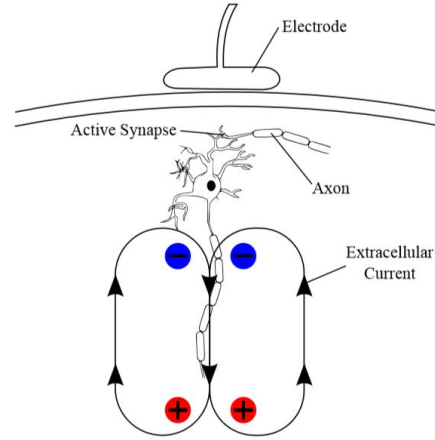


Fig. 3. Electrical dipole measured by the EEG electrode [Burger, 2014]

EEG signal types will be differentiated based on identification and measurement of parameters specific to each signal type. However, the signals recorded by EEG electrodes express not only neural activity of the source located under the electrode, but a sum up of the neural activity run in various brain locations.

EEG is a non-invasive procedure (no need for any device going inside the body) which uses electrodes for measuring the neural activity. A medium size electrode would normally consist in an Ag-AgCl disk, 1 to 3 mm diameter [Teplan, 2002] and is located directly on the scalp. There are various electrodes types, such as further detailed:

- disposable (no gel, and pre-gelled);
- reusable electrodes disks (gold, silver, stainless steel, or steel plate);
- a series of cap and easycap electrodes;
- NaCl electrodes.

Montage will be as per features of EEG data rendering, i.e. or display or on paper. Rendering features would include rendered ordering and channels, as well as recording technical styles (electrode specific) [Libenson, 2013]. Two distinct recording techniques are mainly used, i.e. *bipolar*, and *referential* montage, which somewhat overlap. *Bipolar* montage is a technique which identifies the voltage difference between adjacent electrodes; yet, due to the low proximity of the adjacent electrodes to each other, information is lost [Libenson, 2013]. The *referential* montage compares all of the electrodes with one single reference electrode. The

reference electrode location may be selected so the voltage should be *neutral*. In practice, the reference electrode will be attached to the least noise-prone region [Libenson, 2013].

*International Federation of Societies for EEG and Clinical Neurophysiology* set up a standard for electrodes location, known as *10-20 system* [Forslund, 2012]. Fig. 4 indicates montage in 10-20 system of 21 electrodes, where channel Fz is located on forehead, whereas channel Pz at the back of the head. For instance, if is the movement of the right, respectively of the left, finger, is monitored, electrodes C3 and respectively C4 will be used. The electrodes for the ear lobe (A1 and A2, not indicated) are often used as reference electrodes. For a thoroughly detailed EEG recording, an international 10-5 system was set up, where a number of electrodes are located on the subject's scalp [Forslund, 2012]. Fig. 4, b illustrates an instance of *Geodesic* sensors network with 128 channels, where channel 17 is located on forehead, and channel 82 at the back of the head, whereas Cz acts as a reference electrode. Channels 37, 105 and 16 of the *Geodesic* network are equivalents of channels C3, C4 and Fz.

During the EEG signals recording, it was noted that such signals manifest specific features which vary with the subject's age, as also with the subject being asleep or awake [Sanei & Chambers, 2008]. Based on such features, the brain waves may fall into six categories. Such 6 categories are known as alpha ( $\alpha$ ), theta ( $\theta$ ), beta ( $\beta$ ), delta ( $\delta$ ), gama ( $\gamma$ ), and miu ( $\mu$ ), each expressing a bandwidth of frequencies [Sanei & Chambers, 2008; Baztarrica, 2012]. Table 2.1 indicates each category's frequency margin, as well as a number of mental functions, which are ascertained roles of the frequency margin.

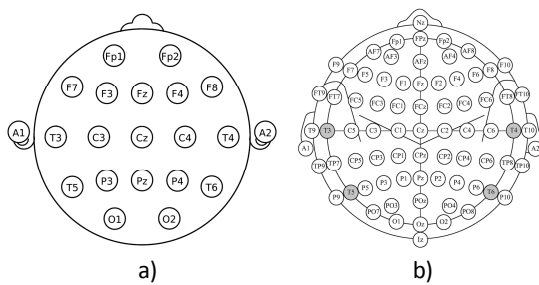


Fig. 4. Electrodes location as per international standards: (a) 10-20; (b) 10-10 [PEERJ, 2016]

There is a number of distinct techniques which measure brain activity. Imaging based on functional magnetic resonance (fMRI), single-photon emission computed tomography (SPECT) which measures secondary functions, as well as metabolism and exchanges of oxygen, blood volume and flow; and positrons emission tomography (PET). [Sanei & Chambers, 2008; Menon & Crottaz-Herbette, 2005].

By such techniques the whole amount of brain activity can be measured; however, due to hemodynamic delay (during which required oxygen level in blood rises) temporal resolution thereof is low: 1 to 6 s [Menon & Crottaz-Herbette, 2005; Ashrafulla, 2012]. EEG technique for measuring brain electrical activity, and magnetoencephalography (MEG), for measuring the magnetic field produced by the brain electrical activity, can be useful only in measuring surface activity, which occurs close to scalp. However, EEG and MEG supply a high temporal resolution, up to 1 ms [Ashrafulla, 2012], an aspect which makes such techniques usual in analysis of brain activity measurement. Magnetic fields are less distorted by the scalp than the electrical fields, thus MEG manifesting a spatial resolution higher than EEG. MEG can detect, however, only the tangential components of the current sources in the brain, whereas EEG detects both the tangential and the radial component [Ashrafulla, 2012].

EEG techniques are used mainly in research, as non-invasive measuring devices for recording the patients' brain activity, such device being used for monitoring comatose patients' brain activity, in order to identify the lesion regions, and in order to predict epileptic seizures [Teplan, 2002]. The most useful usage however, was proven to be the interaction with technology in brain-computer interfaces (BCI). Orders extracted and interpolate in EEG are used to control either a cursor on a display, or an avatar in the virtual space, and such like [McFarland, McCane, David & Wolpaw, 1997]. During EEG recording, noise occurs, which contaminates brain electrical activity (EEG); such noise is known as *artefact* [Libenson, 2012]. *Artefacts* are electrical activities produced outside of the brain, contaminating and/or obstructing relevant brain activity recorded by EEG (see Fig. 5). Such signals can occur in any point of an EEG recording, whereas amplitudes thereof are normally higher than the amplitudes of cortical signals of interest [Libenson, 2012]. The various types of artefacts may be ranked as physiological, respectively and non-physiological.

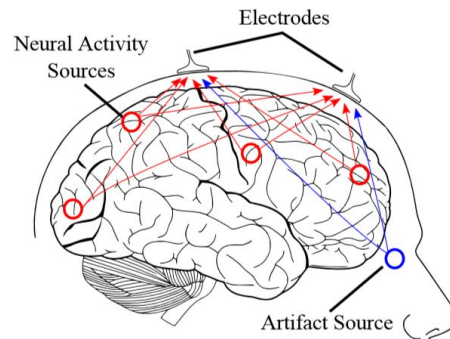


Fig. 5. Recorded neural activity sum up [Burger, 2014]

## 2.2 Dynamics of stimulated brain activity

Experts manifest a worldwide intense preoccupation to highlight dynamic aspects of brain behavior. The highest challenge of these 40 years is undoubtedly the paradigm of the BCI systems, which permit the control of an artificial device; such control is based on features extracted from electrical, magnetic, or other type physical voluntary manifestations, of cortical activity, collected epi- or subdural from cortex or scalp, or in an invasive electrophysiological manner, to be more specific brain waves biosignals intracortically recorded using a unique electrode, or else multi- electrode network [Dornhege, Millán, Hinterberger, McFarland, Müller & Sejnowski, 2007]. Recent studies proved the correlations existing between the EEG bio-signals and actual or imagined moves, as well as between EEG signals and mental loads [Keirn & Aunon, 1990]. Electrical neuronal activity covers a wide frequency bandwidth; thus, monitored brain waves bio-signals are filtered noise-free and in order for the relevant information to be extracted. Finally, such information is decoded and transformed into orders for the device, by synchronous control, or, more efficiently, by self-adjusted or asynchronous control, in order to detect if the subject's move was intended or not. For a number of specific BCI loads, gross brain bio-signal acts as a stimulus, as well as feedback for interface control.

As neural activity signatures, EEG bio-signals can be captured by multiple electrodes EEG devices, inside of the brain, on the cortex brain, or at specific locations on scalp, recordable under various forms. Biosignals are normally presented in the time domain, yet a number of new EEG devices, as further indicated in the case of the NeuroSky headset, are able to apply simple processing methods, as would be Fourier representation for frequencies analyses, a number of which being even equipped with imaging devices for visualizing EEG topographies (spatial maps of brain activity).

Up to present day, several algorithms for EEG bio-signal processing have been developed, including – unlimitedly – time domain analysis methods, frequency domain analysis, spatial domain analysis, and multimodal processing; hence a number of algorithms have been developed for brain waves activity visualization in images which can only be reconstructed by EEG.

In the EEG technique involving a high cortical activity dynamics, two types of systems are normally used: endogenous load based systems, respectively exogenous loads based systems [Dornhege, Millán, Hinterberger, McFarland, Müller & Sejnowski, 2007]. Endogenous load systems, based on spontaneous activity, use brain waves signals which do not depend on external stimuli, and which can be influenced by focusing on specific mental loads. In order to obtain an efficient load recognition system,

a number of focusing attempts on the part of the subject are normally run. Limiting the focusing is a fatiguing mental load, especially for the disabled subjects who may have a hard time getting voluntary control on their brain waves activity; such limiting must be low in order to obtain an efficient load recognition system. Exogenous load systems, based on evoked activity, use brain waves signals which depend on external stimuli. Particularly interesting are the systems based on either P300 (evoked potential) or on SSVEP (steady state visual evoked potentials). Advantages of such potentials consist in being relatively well understood neurophysiologically, and robustly evocable by various subjects. Moreover, such systems do not require training by feedback, as such potentials show *per se*, regardless of the subjects focusing on one single stimulus, or on a number of stimuli presented in randomized order [Hoffmann, Vesin, Ebrahimi & Diserens, 2008].

Over the data acquisition phase, an individual's neural activity is obtained by invasive or non-invasive methods using electrodes. Neural activity recorded is sampled at a selected sampling rate, which is then amplified, by special equipments. Data yielded in bio-signal acquisition are contaminated by artefacts, the reason why such data must be processed, in order to highlight the signal/noise ratio. Such processing grants high standard EEG quality, as required for ranking mental loads.

After the signal/noise ratio is improved, the features as well as the spatial filtering, the measurement of voltage amplitude and the spectral analysis, are extracted in data which codify the message and the subjects' command. Such features can be in time domain (e.g. echo potential amplitudes) and/or in the frequency domain (e.g.  $\mu$  or  $\beta$  rhythms amplitudes) [Forslund, 2003; Wolpaw, Birbaumer, McFarland, Pfurtscheller & Vaughan, 2002].

Both sensorimotor activity and rhythms of the brain waves change ( $\mu$ ,  $\beta$  and  $\gamma$ ), and the potentials related to movement (MRP), the slow cortical potentials (SCP), evoked potential (P300), visual evoked potential (VEP) and response to mental loads, express the more dynamic part of the brain waves activity, very accurately captured in the EEG analysis.

## 2.3 Local EEG model (LEM)

Branch literature illustrates a series of models elaborated for normal and abnormal EEG generation [Sanei & Chambers, 2008]. As a rule, such models are nonlinear. The simplest model consists in a set of simulated neurons, thalamocortical cells type relay and interneurons, embedding physiological and histological limited data, as available at EEG time [Lopes, Hoeks, Smits & Zetterberg, 1974]. Fig. 6 illustrates model LEM, variant Wilson and Cowan [Wilson & Cowan, 1972], which advances a set of equations able to describe overall activity (not

specifically EGG) in a complex of excitatory and inhibitory neurons with a high number of interconnections [Zetterberg, 1973].

Even though the model is per se analogous, all of the blocks are implemented in a discrete form. Such model may consider the major features of one distributed model; it is easy to investigate the resulting change of bandwidth by the influence of the excitatory and inhibitory thalamocortical relay cells and of the interneurons. In the terms of LEM, the EEG rhythms are supposedly generated by distinct nerve populations, which manifest frequency selective features. Such populations are made of interconnected single neurons and are supposedly driven by an aleatory input. The model features, such as neural interconnectivity, response pulse of synapse, and excitation threshold, are expressed in terms of LEM parameters. Changes at such parameters' level produce relevant EEG rhythms.

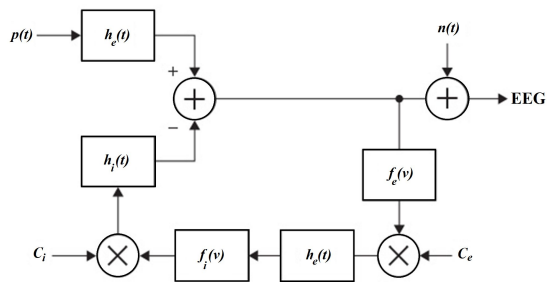


Fig. 6. Local EEG (LEM) model [Wilson & Cowan, 1972; Sanei & Chambers, 2008]

Relay type thalamocortical neurons are expressed by two linear systems manifesting responses to the excitatory impulse  $h_e(t)$ , at upper branch and inhibitory postsynaptic potential, expressed as  $h_i(t)$ . Such system's non-linearity is described as  $f_e(v)$ , expressing a target generator process. Function  $f_e(v)$  can be modified in order to generate EEG signals for various brain abnormalities. Inter-neuronal activity is also expressed by one more linear filter  $h_e(t)$  in the lower branch, which may differ from the first linear system; and by nonlinear function  $be(v)$ .  $C_e$  and  $C_i$  express a number of inter nerve cells, respectively, thalamocortical neurons. An inhibitory neuron's average number of inputs from the excitatory neurons is determined by  $C_e$ , and respective number of inhibitory neurons, for each excitatory neuron, is  $C_i$ . Input  $p(t)$  is supposed to result from the sum up of one series of aleatorilly distributed potentials which drive the circuit excitatory cells, generating a real-time background EEG signal. Such signals from deeper brain sources, at trunk and thalamus level, are part of the action, or spontaneous activation of the center nervous system (SNC), [Sanei & Chambers, 2008].

The mathematical relation advanced by Wilson and Cowan for modeling each postsynaptic potential  $h_e$  and  $h_i$  is

$$h_e(t) = A[e^{-a_1 t} - e^{-a_2 t}] \quad (1)$$

$$h_i(t) = B[e^{-b_1 t} - e^{-b_2 t}] \quad (2)$$

where  $A$ ,  $B$ ,  $a_k$ , and  $b_k$  are constants which control pulse waves shape. Membranes potentials are correlated to the impulses density along axons by threshold (static) functions  $f_e$  and  $f_i$ . Such functions are, normally, non-linear; yet, for smooth operation, such are taken to be linear for each short time interval. The model here described manifests a single EEG channel, presenting no modeling of the inter-channel relations. For a complex and undoubtedly much more accurate approach, a model must be defined which allows for simulation of a system by generating an EEG multichannel; such aspect is still being studied.

#### 2.4. EEG Parameters

In (semi)automatic processing procedures of EEG signals, the fact is considered that, in information terms, EEG parameters are *temporal, statistical by amplitude and frequency related*. The temporal parameters follow the intersections with the axis and the amplitude extremes (the variance maximum-maximorum vs. minimum-minimorum) per time unit, respectively the first and the second order temporal means: the average value, the mean square value, the dispersion, the mean square deviance, the cross correlation and the autocorrelation functions and coefficients, and the crosscovariance and autocovariance functions. If histogram distribution is Gaussian, standard average and variance will be manifested. For non-Gaussian distributions, useful data are provided by skewness and kurtosis. Skewness measures the shifting angle from normal distribution symmetry, as against basic line. Values other than zero of such parameter indicate presence of monophasic episodes in EEG.

*Statistical parameters of amplitude are determined on histogram, based on density probability (second order histogram). The probability density diagram computes the average value, the median (mean value of the x variable domain) and the mode (highest density point).*

##### 2.4.1 Power spectral density

*Frequency parameters imply a frequency analysis based on the amplitude specters supplied by the Fourier transform and on the power specters. Frequency parameters highlight EEG specific rhythms, whose frequency distribution is associated with psychophysical states of the subject. Thus, data*

regarding the fatigue level are supplied by the EEG power signal, yielded by the zone below the spectral power density function, whereas the specific pathological manifestations are associated with frequency bandwidth shifting. [Hariton, 2009].

Power spectral density is power distribution in bandwidth B of signal x(t). Here are the relations for the power signal with center frequency f<sub>0</sub> in bandwidth B, respectively for power spectral density:

$$P(f_0, B) = \lim_{T \rightarrow \infty} \frac{1}{T} \int_0^T |x(t)|^2 dt \quad (3)$$

$$S(f_0)df = \left( \frac{dP(f)}{df} \right)_{f=f_0} df \quad (4)$$

(3) and (4) express that, over a narrow bandwidth Δf, around f<sub>0</sub>, if Δf → 0 ⇒ P(f<sub>0</sub>, B) → S(f<sub>0</sub>). The narrower Δf is, the closer average power over such bandwidth gets to spectral density.

EEG spectral analysis is normally run with a system consisting in a filter which allows for crossing the bandwidth with f<sub>0</sub> as a pivoting point, a square detector and an integrator. Such analyzers can be type parallel, series (scanner), dispersive filter, time compression and Fourier.

Fourier analyzer (see Fig. 7) is made of a correlator and a Fourier transform. The Fourier transform contains two multipliers, the weighing functions memories, the sin and cos memories, a numerical integrator and a processing block.

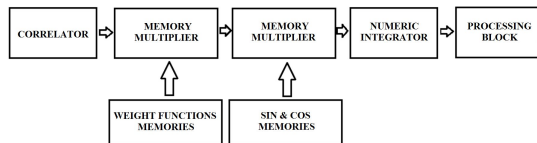


Fig. 7. Fourier analyzer [Hariton, 2009].

Computing relation will be inferred by Wiener-Hincin theorem:

$$S_{xx} = \int_{-\infty}^{\infty} C_{xx}(\tau) e^{-j\omega\tau} d\tau \quad (5)$$

where C<sub>xx</sub> is the autocorrelation function of an EEG signal.

The autocorrelation function is extracted from the memory and multiplied by the weighing functions, in order to smooth the specter for the wider bandwidth signals. Sin and cos memories implement the exponential function. At processing block output point, the real and the imaginary components, the module and the phase of the Fourier transform will be supplied. Analysis of an EEG signal spectral power supplies quantitative information about EEG distribution in frequency, which is easily done by means of the Fast Fourier Transform (FFT) algorithm.

Based on the EEG/FFT correlation function, the power specter will be deduced after the relation:

$$P(f) = R_e^2[X(f)] + I_m^2[X(f)] \quad (6)$$

where X(f) is EEG signal Fourier transform along a channel.

Coherence quantifies the connection among various EEG channels, value thereof being yielded by relation:

$$Coherence = \frac{cross\ specter}{\sqrt{PX(f) - PY(f)}} \quad (7)$$

The cross specter is yielded by the multiplication X(f) Y\*(f) where X(f) and Y(f) the EEG signals' Fourier transforms along two channels, whereas (\*) is the complex conjugate.

EEG signal phase is yielded by the polar representation angle thereof, coherence being a complex number. The phase may indicate brain waves activity interactions recorded in various cerebral surface areas.

Linear spectral analysis of EEG signals implies multichannel EEG signals acquisition, computation of power spectral density (by FFT), of the cross specter, of coherence and of phase relations.

#### Example 1:

Fig. 8 illustrates a diagram of average power spectral densities, corresponding to measurements, by an EEG device, run on 20 subjects, no exogenous stimulation.

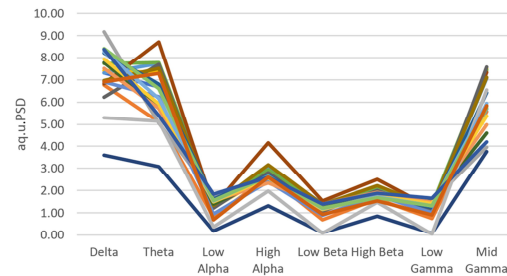


Fig. 8. Diagram of the average power spectral densities over the EEG bandwidth

As mediating the values of power spectral densities, stabilization of patterns may be noted, similar in terms of shape, however highly specific for each subject assessed. Mediating the power spectral densities values in each EEG bandwidth is needed in order to run comparative studies, with values yielded by other type measuring devices.

#### 2.4.2 Inferential function Ψ<sub>EEG</sub>

The association of mental states with specific levels of power spectral density, or with specific structures of such parameters, by means of an integrative approach, may lead to identification of psychophysical patterns. In such case, relations

amongst the physiological factors that must be followed as temporal and spatial reactions profiles are: *one-to-one* relation; *null* relation; *one-to-multiple* relation; *multiple-to-one* and *multiple-to-multiple*. Relations *multiple-to-one* and *multiple-to-multiple* can be simplified by redefining the factor signifying an element in the psychological or physiological domain. The invariant expresses an overall isomorphic (*one-to-one*) association. Such methods' development and application by intrinsic physiological recording can contribute to the progress of research of social and psychological phenomena, by measuring the solved previously contested predictions, the highlighted phenomenons previously unnoticed becoming noticeable, while conclusions previously accepted may start being questioned [Cacioppo & Tassinary, 1990].

*Correlation of EEG specific rhythms with the psychophysical states of a subject* implies determination of biunivocal relations between *power spectral density* on each bandwidth and categories of psychological indices, taken to be inferential channels. On such terms, each channel  $i$  manifests an inference specific to a bandwidth  $j$ . That is why it is important to know in what way, the average *spectral power density*  $\overline{S}_B$  on a bandwidth  $j$ , corresponds by inference  $\gamma_{EEG}$  to psychological aspects meaningful along an analysis channel  $i$ . Here is the expression of quoted relations:

$$S_{ij} = \begin{pmatrix} \chi_{11} \overline{S}_{B1} & \chi_{12} \overline{S}_{B2} & \cdots & \chi_{1j} \overline{S}_{Bj} \\ \chi_{21} \overline{S}_{B1} & \chi_{22} \overline{S}_{B2} & \cdots & \chi_{2j} \overline{S}_{Bj} \\ \cdot & \cdot & \cdot & \cdot \\ \chi_{i1} \overline{S}_{B1} & \chi_{i2} \overline{S}_{B2} & \cdots & \chi_{ij} \overline{S}_{Bj} \end{pmatrix} \quad (8)$$

for  $(\forall)i = \overline{1, n}; (\forall)j = \overline{1, n}$ , where  $\chi_{ij}$  is a function which expresses the impact of average *power spectral density*  $\overline{S}_B$  on a bandwidth  $j$  along channel  $i$ , so that relation between  $\overline{S}_B$  and  $\gamma_{EEG}$  will be:

$$\gamma_{EEGij} = \beta \chi_{ij} \overline{S}_{Bj} \quad (9)$$

where  $\beta$  is a  $\tau / |\overline{S}_{Bn} - \overline{S}_{B1}|$  scale factor,  $\tau$  is a technological constant, while  $\overline{S}_{Bn}$  and  $\overline{S}_{B1}$  are power spectral densities over bandwidth  $n$  and  $1$ .

Considering that the psychophysical inference ratio implies the inferential reproduction of the  $\Psi_{EEGij}$  psychological functions table, the inferential relation between factors may be determined starting from (9), as further indicated:

$$\psi_{EEGij} = \rho_{EEGi} \gamma_{EEGij} \quad (10)$$

where  $\rho_{EEGi}$  is the efficiency with which EEG biosignal of spectral power density  $\overline{S}_{Bj}$  may produce an inference along channel  $i$ :

$$\rho_{EEGi} = m \frac{\sum_{j=1}^n \chi_{ij} \overline{S}_{Bj}}{\sum_{i=1}^m \sum_{j=1}^n \chi_{ij} \overline{S}_{Bj}} \quad (11)$$

a relation based on which *EEG* final form  $\psi_{ij}$  *inferential index* may result:

$$\psi_{EEGij} = \frac{m\tau}{|\overline{S}_{Bn} - \overline{S}_{B1}|} \frac{\chi_{ij} \overline{S}_{Bj} \cdot \sum_{j=1}^n \chi_{ij} \overline{S}_{Bj}}{\sum_{i=1}^m \sum_{j=1}^n \chi_{ij} \overline{S}_{Bj}} \quad (12)$$

Relations (9) and (10) connect the inferential function with the average *spectral by power density*  $\overline{S}_{Bij}$  so that the inferential function *per se* may be seen as a time function,  $\psi_{EEG}(t)$ , behavior thereof being analyzable in the aleatory processes paradigm.

In order to express the inference of the psychic aspects in the neural processes, for local model (LEM) advanced by [Wilson & Cowan, 1972] we will consider function  $\psi_{EEG}(t)$  as an adjustment function (see Fig. 9).

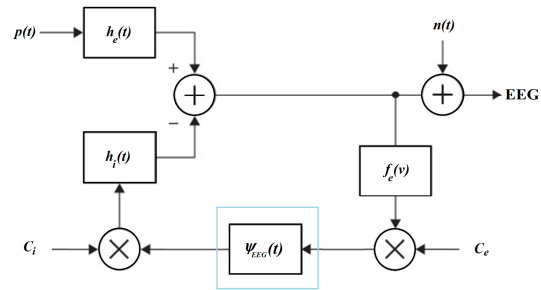


Fig. 9. The inferential function in LEM model

In such case, the role of the linear filter  $h_e(t)$  is granted by component  $\chi_{ij}(t)$ . For each inferential function a random experience is considered, the result being seen as one of the possible result variants thereof.  $\Gamma$  is the samples space made of the multitude of possible results. Hence the inferential function will actually be a collection of signals usual in the time continuum, known as trajectories. To each point  $\gamma$  in space  $\Gamma$ , a function will be associated, of limited duration in time:

$$\Psi(t, \gamma), -T \leq t \leq T \quad (13)$$

duration 2T being the observation interval. If point  $\gamma$  is set,  $\gamma = \gamma_j$ , time function  $\Psi(t, \gamma)$  is a sample function:

$$\psi_j = \Psi(t, \gamma_j) \quad (14)$$

For a multitude sample functions, type:  $\{\psi_j(t) | j = 1, 2, \dots, n\}$ , setting  $t = t_k$ , set:

$$\{\psi_1(t_k), \psi_2(t_k), \dots, \psi_n(t_k)\} = \{\Psi_1(t_k), \Psi_2(t_k), \dots, \Psi_n(t_k)\} \quad (15)$$

is an aleatory variable [Papoulis, 1977]. Thus, the process will be seen as a set of aleatory variables, indexed by time:  $\{\Psi_j(t, \gamma)\}$ , where in order to simplify designations,  $\gamma$  is given up, noting the process  $\Psi(t)$ .

For a strictly stationary aleatory process  $\Psi(t)$  average thereof is:

$$\mu_x(t) = E\{\Psi(t)\} = \int_{-\infty}^{\infty} \psi p_{\Psi(t)}(\psi) d\psi \quad (16)$$

where under the integral there is a repartition density of an inferential variable  $\Psi(t)$  for  $t$  set [Porat, 1994]. When the process is strictly stationary, the relation will be:

$$\mu_x(t) = \mu_x \quad (17)$$

For two set times,  $t_1$  and  $t_2$ , and a repartition density common with inferential variables  $\Psi(t_1)$  and  $\Psi(t_2)$ , type:  $p_{\Psi(t_1)\Psi(t_2)}(\psi_1, \psi_2)$ , the average of the aleatory variables produced will be written, as associated to each pair  $(t_1, t_2)$ ; such average value is known as *statistical correlation function* of an aleatory signal:

$$\begin{aligned} \mu_{\Psi(t_1)\Psi(t_2)} &= E\{\Psi(t_1)\Psi(t_2)\} \\ &= \int_{-\infty}^{\infty} \int_{-\infty}^{\infty} \psi_1 \psi_2 d\psi_1 d\psi_2 \end{aligned} \quad (18)$$

For a strictly stationary aleatory process, designations being:

$$\mu_{\Psi(t_1)\Psi(t_2)} = R_{\Psi}(t_1, t_2) \quad (19)$$

We will have for  $p_{\Psi(t_1)\Psi(t_2)}(\psi_1, \psi_2)$  only one dependence on the difference  $t_2 - t_1$ , not on absolute time values. In such case, (19) becomes:

$$R_{\Psi}(t_1, t_2) = R_{\Psi}(t_2 - t_1) = R(\tau), \forall t_1, \forall t_2 \quad (20)$$

a function which illustrates a maximum in origin [Stoica & Moses, 2005].

A spectral analysis of aleatory signals can be run on statistical and energy criterions, as per theorem Wiener-Hincin; statistical correlation function determined above, associated with the spectral power distribution, yields a Fourier pair.

### Example 2.

We further advance, for an illustration, a computation of the values for a set of *EEG inferential indices*, in average values of the spectral power densities of the EEG bandwidth, for a psychophysical inferential system, dimension  $i \times j$ , where  $i = 7$  and  $j = 8$ :

Table 1 indicates function  $\chi_{ij}$  values, as computed for an EEG bandwidth specter, values  $\bar{S}_{B_j}$ , as well as efficiency with which inference is produced along each channel. Computation of the EEG inferential indices set was run for  $m=7$  and  $\tau=75$ .

Table 1: Experimental values  $\bar{S}_B$ ,  $\chi_{ij}$  and  $\rho$

|             | Delta<br>(eq.u.PSD) | Theta<br>(eq.u.PSD) | Low Alpha<br>(eq.u.PSD) | High Alpha<br>(eq.u.PSD) | Low Beta<br>(eq.u.PSD) | High Beta<br>(eq.u.PSD) | Low Gamma<br>(eq.u.PSD) | Mid Gamma<br>(eq.u.PSD) |             |
|-------------|---------------------|---------------------|-------------------------|--------------------------|------------------------|-------------------------|-------------------------|-------------------------|-------------|
|             | <b>73.11</b>        | <b>66.75</b>        | <b>14.41</b>            | <b>29.09</b>             | <b>12.20</b>           | <b>19.59</b>            | <b>14.63</b>            | <b>58.37</b>            | $\rho$      |
| $\chi_{1j}$ | 0.40                | 0.49                | 1.27                    | 1.05                     | 1.30                   | 1.19                    | 1.27                    | 0.62                    | <b>1.00</b> |
| $\chi_{2j}$ | 0.41                | 0.50                | 1.29                    | 1.07                     | 1.32                   | 1.21                    | 1.29                    | 0.63                    | <b>1.02</b> |
| $\chi_{3j}$ | 0.41                | 0.51                | 1.30                    | 1.08                     | 1.33                   | 1.22                    | 1.30                    | 0.63                    | <b>1.02</b> |
| $\chi_{4j}$ | 0.40                | 0.50                | 1.28                    | 1.06                     | 1.31                   | 1.20                    | 1.28                    | 0.62                    | <b>1.01</b> |
| $\chi_{5j}$ | 0.41                | 0.50                | 1.30                    | 1.08                     | 1.33                   | 1.22                    | 1.29                    | 0.63                    | <b>1.02</b> |
| $\chi_{6j}$ | 0.39                | 0.48                | 1.23                    | 1.02                     | 1.27                   | 1.16                    | 1.23                    | 0.60                    | <b>0.97</b> |
| $\chi_{7j}$ | 0.39                | 0.48                | 1.23                    | 1.02                     | 1.26                   | 1.15                    | 1.22                    | 0.60                    | <b>0.96</b> |

In terms of (12), *psychophysical tensor*  $\Psi_{EEG}$ , for dimension 7x8 becomes:

$$\Psi_{78} = \frac{m\tau}{|\bar{S}_{B_8} - S_{B_1}|} \begin{pmatrix} \chi_{11}\bar{S}_{B_1} \sum_{j=1}^8 \chi_{1j}\bar{S}_{B_j} & \chi_{12}\bar{S}_{B_2} \sum_{j=1}^8 \chi_{1j}\bar{S}_{B_j} & \chi_{18}\bar{S}_{B_8} \sum_{j=1}^8 \chi_{1j}\bar{S}_{B_j} \\ \sum_{i=1}^7 \sum_{j=1}^8 \chi_{i1}\bar{S}_{B_i} & \sum_{i=1}^7 \sum_{j=1}^8 \chi_{i2}\bar{S}_{B_i} & \sum_{i=1}^7 \sum_{j=1}^8 \chi_{i8}\bar{S}_{B_i} \\ \chi_{21}\bar{S}_{B_1} \sum_{j=1}^8 \chi_{2j}\bar{S}_{B_j} & \chi_{22}\bar{S}_{B_2} \sum_{j=1}^8 \chi_{2j}\bar{S}_{B_j} & \chi_{28}\bar{S}_{B_8} \sum_{j=1}^8 \chi_{2j}\bar{S}_{B_j} \\ \sum_{i=1}^7 \sum_{j=1}^8 \chi_{i1}\bar{S}_{B_i} & \sum_{i=1}^7 \sum_{j=1}^8 \chi_{i2}\bar{S}_{B_i} & \sum_{i=1}^7 \sum_{j=1}^8 \chi_{i8}\bar{S}_{B_i} \\ \chi_{71}\bar{S}_{B_1} \sum_{j=1}^8 \chi_{7j}\bar{S}_{B_j} & \chi_{72}\bar{S}_{B_2} \sum_{j=1}^8 \chi_{7j}\bar{S}_{B_j} & \chi_{78}\bar{S}_{B_8} \sum_{j=1}^8 \chi_{7j}\bar{S}_{B_j} \\ \sum_{i=1}^7 \sum_{j=1}^8 \chi_{i1}\bar{S}_{B_i} & \sum_{i=1}^7 \sum_{j=1}^8 \chi_{i2}\bar{S}_{B_i} & \sum_{i=1}^7 \sum_{j=1}^8 \chi_{i8}\bar{S}_{B_i} \end{pmatrix} \quad (21)$$

The  $\Psi_{EEG}$  values are indicated in Table 2, as recorded on a standard 75 to 265 inferential units scale.

**Table 2:**  $\Psi_{EEG}$  experimental values

| Canalul | $\Psi_{11}$<br>[u.mf.] | $\Psi_{12}$<br>[u.mf.] | $\Psi_{13}$<br>[u.mf.] | $\Psi_{14}$<br>[u.mf.] | $\Psi_{15}$<br>[u.mf.] | $\Psi_{16}$<br>[u.mf.] | $\Psi_{17}$<br>[u.mf.] | $\Psi_{18}$<br>[u.mf.] |
|---------|------------------------|------------------------|------------------------|------------------------|------------------------|------------------------|------------------------|------------------------|
| 1       | 148.30                 | 167.42                 | 93.02                  | 155.62                 | 80.81                  | 118.82                 | 94.20                  | 183.31                 |
| 2       | 153.26                 | 173.02                 | 96.14                  | 160.83                 | 83.51                  | 122.79                 | 97.35                  | 189.44                 |
| 3       | 155.50                 | 175.56                 | 97.54                  | 163.18                 | 84.74                  | 124.59                 | 98.78                  | 192.21                 |
| 4       | 150.44                 | 169.84                 | 94.37                  | 157.87                 | 81.98                  | 120.53                 | 95.56                  | 185.95                 |
| 5       | 154.83                 | 174.79                 | 97.12                  | 162.47                 | 84.37                  | 124.05                 | 98.35                  | 191.38                 |
| 6       | 140.01                 | 158.06                 | 87.82                  | 146.92                 | 76.29                  | 112.17                 | 88.93                  | 173.06                 |
| 7       | 138.35                 | 156.19                 | 86.78                  | 145.18                 | 75.39                  | 110.85                 | 87.88                  | 171.01                 |

### 2.4.3 Acquisition of EEG biosignals

In current practice, obtainment of a MRI imaging is costly, whereas development of an application for command and remote control of a movement based on such patterns implies an elaborated system, for acquiring, processing and defining a stimulus induced signal, a system which in terms of sizing and collateral utilities goes beyond the application's optimal framework. A markedly lower cost alternative, yet capable of versatile signals form analyses, is the acquisition of EEG signals making use of last generation dedicated headsets.

Neuro Sky MindSet headset (see Fig. 10) is a device able to take over EEG biosignals at forehead level, by means of three dry electrodes, reproducing neurocortical activity in brain waves power specters, and calibrated to supply expression in biosignals of attention, meditation and blinking.



Fig. 10: Neuro Sky MindSet headset.

NeuroSky devices can measure multiple simultaneous mental states. Brain waves physics is nearly identical with the physics of the sound waves, where a single microphone may increase the complexity of a concert. All of the electrical devices, computers included, bulbs, wall sockets and such like, emit a specific environmental noise level.

Such noise is often strong enough to impact the brain waves. As result, EEG lab devices will take over aleatory readings, when the reference electrode, as well as the primary electrode, are connected to an object which does not emit brain waves. In the past, the EEG traditional devices went round such problem by measuring the brain waves in strictly controlled medium, in order not to interfere with EEG signals. A medical conductivity gel is used for increasing brain waves EEG signals. As EEG devices migrate from the lab to wide scale usage, most people no longer have a space with no electronic

interference, and do not agree to get conductive gel on scalp each time they use an EEG device. Based on sensors, no gel and no noise-prone medium, NeuroSky procedures lower such risks to a minimum [NSKY, 2011].

Part of the NeuroSky devices involves noise annulment. Signal amplification makes gross brain waves signal stronger. Filtering protocols oust the frequencies of noise known, such as muscular, pulse and electrical devices noise. *Notch* filters oust the grid electrical noise, which varies 50 to 60Hz, function of each country's specific regulations. Filtering technology is a top preoccupation of NeuroSky R&D, and future products will refine today's capacities, yet perfectible as of now.

Extrapolation of the EEG brain waves signals into *noises* makes use of a reference point and of a grounding electrical circuit. By grounding, body voltage is brought at the same level with the headset voltage.

The reference point is used for extracting the common environmental noise by a rejection process [NSKY, 2011]. The ear lobe is an area which feels environmental noise the same way the NeuroSky frontal sensor does, yet with minimum neuronal activity. It is therefore important, for accurate operation, that the headset should be connected to ear as carefully as possible. For validation, NeuroSky ran measurement tests on EEG dry sensor, by comparing EEG signals begot from a dry sensors system, with Biopac system signals, a well known EEG wet electrodes system, widely used in medical and research applications.

EEG signals were simultaneously recorded, by the NeuroSky system and the Biopac system. The two systems' electrodes were located at the same places, together, as close as possible yet not interfering. Dry gold plated electrodes were used for the NeuroSky system, whereas for Biopac disposable wet electrodes were used, with AgCl based gel. EEG signals were recorded for various stances, the subject under testing being, on turns, relaxed, respectively alarmed, or focusing, or generating artefacts by blinking [NSKY, 2011].

The gross EEG signals taken over with dry electrode NeuroSky system were compared with the signals begot from the wet electrode Biopac system. FFT's were run in order to compare the EEG signal features, especially the power spectrum. The results indicate that the NeuroSky system EEG signals are compatible with the Biopac system signals. Biopac system EEG's manifest a noise somewhat higher in the low frequency bandwidth. As a result, the NeuroSky system is more resistive to noise. The NeuroSky system even manifests advantages when used environmentally, as well as for applications for general use goods.

NeuroSky also developed a proprietary algorithm known as *eSense*, for the detection of mental states

starting from the frequency specters of various type brain waves.

Based on the *eSense* proprietary algorithms, NeuroSky devices can detect, at a quite refined level, states such as *Attention* and *Meditation*. Each second, the headset computes and supplies *eSense* measurements for *Attention* and *Meditation*. Whenever the algorithm detects information apparently incorrect due to noise, respective

measurement is rerun. In order to tell apart the subject's mental states, NeuroSky device can run measurements of *power spectral density* (PSD) over the 1 to 50 Hz bandwidth. Power measured over such bandwidth interval was integrated by extracting the signal with the higher accuracy, then scaling it standard, as measurements with a high energy variation could be read as erroneous reflections of mental states [NSKY, 2011].

### 3. EDA Biosignals

#### 3.1 EDA phenomenology in psychophysiology

Part of the peripheral nerve system, the Autonomic Nerve System (ANS) acts firstly as a regulation function, with a basic role in granting homeostasis.

Changes manifested in ANS activity can also be evaluated by measurements of electrodermal activity (EDA), which has been widely used as a traditional method in psychological research. In such terms, a number of authors [such as Christie, 1981; Turpin & Clements, 1993; Boucsein, 2012] mainly focus on interpreting information as related to electrodermal activity (EDA). The electrodermal response consists in the electrical features changes of an individual's skin, due to interaction among environmental factors, size and psychophysical state.

Normally, the variations in skin resistance and conductance are targeted. The electrodermal response principle is basic to a number of technical implementations on measuring systems of psychophysical aspects, being used for measuring variables specific to the polygraph as well.

Among the number, implementations can be quoted which measure psychogalvanic reflex [Mayer, 1974]; which monitor an individual's psychophysical state [Korenman, 2000]; which visualize psychophysical parameters, making use of an computer assisted interactive bioreactor multimedia system [Fisslinger, 1998]; which evaluate fast psychological profiles [Grigore, 2013] and other such like.

An electrodermal response occurs when two electrodes applied on skin manifested a low enough potential difference for the experiment to be non-invasive. Between such electrodes, an electrical

current occurs on epidermal region, based on which reactive phasic skin conductance (SCR, information carrier) can be measured, [Grigore, 2014]. In the absence of such electrical current, tonic basal conductance (SCL) is manifested. Edelberg distinguishes between individuals electrodermally labile, vs. stabile [Edelberg, 1968].

Such feature may correlate with a series of inferential variables in psychophysiology, differentiation being possible among the individuals' features based on such electrodermal lability and stability.

In terms of the phasic aspect, epidermal conductance is the effect of the eccrine sweat glands activity: when such gland secretes abundantly, phasic conductance changes manifest; respectively, when humidity is absorbed, conductance returns to basic values [Boucsein, 2012]. Thus, sweat glands behavior can be seen as similar to resistance, whose values, the reverse of conductive behavior, drop when humidity is maximum, respectively go up when humidity falls to normal values; the solution quantity secreted by the glands, respectively the number thereof evaluated simultaneously, varies inversely with the amplitude of conductance change.

Sweat glands activity expresses actions such as of brain trunk reticular formations, of hypothalamus, of limbic system and of motor cortex [Bloch, Roland, Eric & Alain, 2006]. A complex diagram of the way in which the neural control acts on sweat glands activity is advanced by [Wang, 1964] (see Fig. 11).

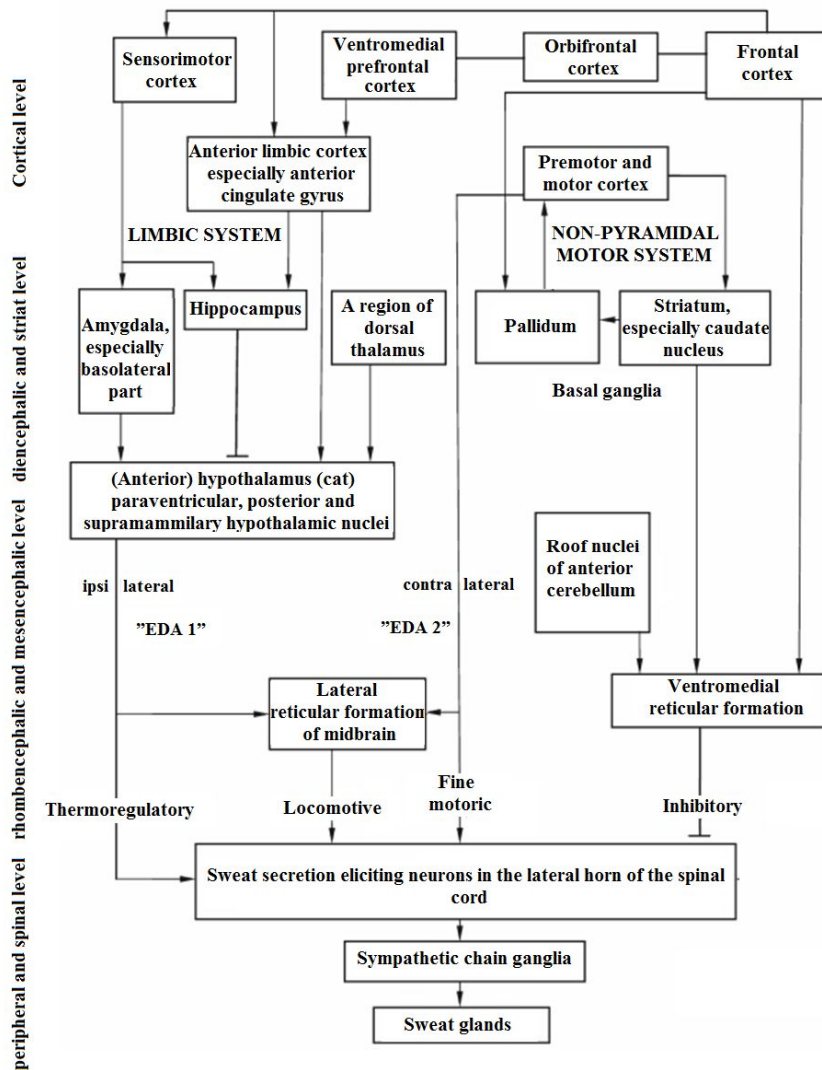


Fig. 11: Conceptual *electrodermal phenomenon* [Wang, 1964; Boucsein, 2012]

As indicated in the block diagram above, there are two pathways by which the electrodermal response is induced, at nerve center system (NCS) level: first (EDA 1), impact limbic system by the thermoregulatory hypothalamic region, involving the amygdala, especially the basolateral side, the hippocampus, a region of dorsal thalamus, anterior hypothalamus, as well as posterior and supramammillary paraventricular hypothalamic nuclei; the second pathway (EDA 2), by contralateral impact from the motor and premotor cortex, respectively basal ganglionic region, i.e. basal ganglia, caudate nucleus, putamen, and globus pallidus.

In order to obtain quantitative measurements, passing from such block diagram to an experimental model will consider especially the theory form of an EDA biosignal, the way (spontaneous vs. stimulated) in which such signal can be obtained, the sensors

type used and, last but not least, such biosignals measuring techniques, in direct vs. alternating current.

Electrodermal response behavior in direct current and alternating current will be further analyzed.

### 3.2 EDA biosignals in direct current

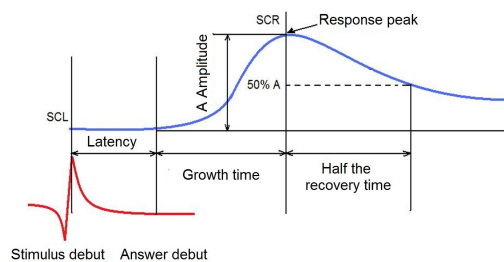


Fig. 12: EDA signal [Grigore, R1, 2014]

Fig. 12 illustrates the theory form of an EDA type biosignal.

In view of running acquisition of EDA biosignals, definitions used are as further detailed and abbreviated:

SRR = skin resistance response;

SRL = skin resistance level (in the range  $1k\ \Omega$  to  $1M\ \Omega$ ); transitory responses, related to sudden changes in psychological state, are of  $100\ \Omega$  order);

SCR = phasic conductance (skin conductance response, expressing conductance transitory changes);

SCL = tonic conductance; skin conductance level, expressing SN (sympathetic nerve) excitation level;

SPR = skin potential response;

SPL = skin potential level.

SRR and SCR are equivalent; hence, SRL and SCL are also equivalent. While SRR, SCR, SRL and SCL, by being exosomatic, depend on an external current source, SPR and SPL (endosomatic) do not, the reason why the common EDA amplifiers are inadequate for SPR and SPL measurement [Edelberg, 1968; Boucsein, 2012].

By processing the acquisition data of electrodermal activity, such parameters are extracted as further detailed:

- amplitude, expressed in micro Siemens ( $\mu S$ ), as yielded by the difference between SCR response maximum level and SCL at the time external stimulus is applied;
- latency (some 3 seconds) expresses duration between stimulus application time and SCR response occurrence time;
- duration of conductance rise is the time taken by rising slope to be covered up to maximum SCR (1 to 3 seconds);
- comeback semi-duration is recorded at the maximum time SCR is touched, up to 50% amplitude level (2 to 10 seconds);
- phasic stadium shift away from the tonic;
- EDA analysis related to event;
- Response expression in skin conductance [Edelberg, 1968; Christie, 1981].

NB. In such terms, direct current used for EDA will not go beyond  $50\ \text{mA}/\text{cm}^2$ .

#### Fowles' model

In 1974, Fowles designed an electrodermal response model in direct current, which he reconfirmed in 1986 (see Fig. 13).

In absence of quantitative data to support the circuit, or quantify any of the factors implied, such model is useful only qualitatively. However, Fowles manages to pertinently structure the electrical representation of connected factors, respectively sweat glands resistance ( $R_1$  and  $R_2$ ), sweat gland wall

resistance ( $R_3$  and  $R_4$ ), horn layer resistance  $R_5$ , the voltage values along duct ( $E_1$  and  $E_2$ ) and horn layer voltage  $E_4$ . As per model advanced by Fowles,  $E_1$  and  $E_2$  are due to ionic dissimilar levels voltage in duct, as well as to selective ionic permeability [Boucsein, 2012].

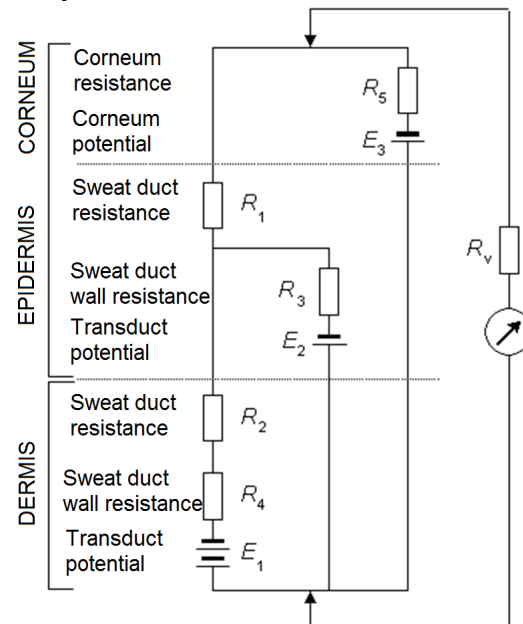


Fig. 13. Electrodermal system equivalent circuit, as advanced by Fowles [Fowles, 1986]

By hydrostatic pressure built up, membranes channel depolarize. Such depolarization makes for higher permeability to ionic flow, as well as for lower  $R_3$  and  $R_4$ .  $E_3$  is the horn layer potential, the potentials meeting location. By hydration of the horn layer,  $R_5$  value falls.

A possible script for the whole reactive process may be described as further detailed:

- if stimulus application implies rest start conditions, at first by sweat response (which rises sweating in ducts)  $R_2$  slightly lowers; duration of such process occurrence is in latency range;
- for a low EDR response,  $R_1$  and  $R_2$  are not affected, respectively SCR does not change;
- with a high EDR response, sudation is extended to horn layer as well, lowering both  $R_2$  and  $R_1$ ;
- a high enough response leads to horn layer hydration, hence a lower  $R_5$ ;
- when the EDR response is quite high, hydrostatic pressure built up in duct will activate the epidermal duct membranes, which will lower  $R_3$ .

In SP potential recordings, potential measured is taken to express, mainly, skin potential - respectively  $E_3$  minus voltage drop in  $R_5$ . Factors considered include Na reabsorption along the duct walls, by active transport, which generates high negative lumen potentials. The effect thereof on measured potentials depend on the relative values of  $R_1$ ,  $R_2$ , and  $R_4$  (low  $E_1$  values rising for surface

measuring, low  $R_5$  values lowering such measuring [Edelberg, 1968]).

With modest responses in case the horn layer is relatively not hydrated, high lumen negative potential and  $R_2$  drop, plus chance  $R_1$  drop, cause a negative monophasic SPR. High responses which trigger membrane response and  $R_3$  marked rapid drop, result in negative measured potential falling, possibly in a positive component, too, if ducts are already filled.

Immediate response to a specific stimulus was experimentally proven to be nearly indistinguishable from spontaneous SCR activity. Such problem was solved using a 1 to 5 s response window, post stimulus, within which the signals were accepted. At a 7.5/min spontaneous SCR rate, the drop in a similar spontaneous SCR is by 50%. For more accurate discrimination, the window must be even narrower.

The advantages of using conductance in direct current consist in concept simplicity, in there existing no skin capacitance, and in numberless quotes to topic existing in the field literature.

Shortcomings would be as further detailed: up to 50 mA/cm<sup>2</sup> limit, intervention by change in the electromotor voltage generated in circuit on electrodes, as well as in skin (electro-osmosis, sweat channels filling up, membranes potentials, skin electrolysis and irritation); usage of bipolar electrodes take data to come from two skin different locations; hence measuring regions are unequal, the reason why conductance in the direct current is improper for physiological research.

### 3.3 EDA biosignals in alternating current.

In the case of conductive media, the load carriers can be the electrons for metals, or the free ions in suspension (in solution) for the biological tissues. If a direct current passes through an ionized solution, (which also happens in Fowles' model), a polarization phenomenon occurs, which can cause the tissue to warm up to self-destruction, in limit cases. Gildemeister was among the first to go round such inconvenient, by using alternating current and by measuring total opposition to passage thereof through a tissue [Gildemeister & Kaufhold, 1920; Lawler, Davis & Griffith, 1960].

In such case, *impedance* is the manifested feature related to physiological activity of tissues subjected to alternating current. Measuring impedance  $Z$  on a biological tissue involves both tissue electrical resistance  $R$ , and capacitive reactance  $X_c$  thereof, after the relation  $Z^2 = R^2 + X_c^2$ . In terms of physics, resistance expresses a conductor's opposition to alternating current, basically the same in biological tissues and in nonbiological conductive materials [Kay, Bothwell, & Foltz, 1954; Nyboer, 1959], whereas biological tissue capacitive reactance is caused by the extra opposition to alternating

current, by the capacitive (stocking) effect of bilipidic cell membranes, of the tissue interfaces and of the structural features [Baker, 1989; Barnett & Bagnò, 1936; Schwan & Kay, 1956].

Membranes acts as dielectric, or as an insulator which sets apart the extracellular and the intracellular fluids, behaving as reinforces of the biological condenser [Grigore & Moldovan, 2015].

With the alternating current (similarly to direct current case) skin humidity is a conditional factor for penetration into organism. The low (under around 5.000 Hz) sinusoidal frequencies are carried only through the conjunctiva tissue of the body [Ivorra & Aguilo, 2001, Ivorra & Rubinsky, 2007], the higher frequencies penetrating the cell outer layers. In case of using rectangular signals, higher frequency harmonics manifest, able to penetrate the cell even if basic frequency is low.

Authors such as Boucsein, Schaefer and Neijenhuisen maintain that electrodermal recording exosomatic techniques consider prevailingly the tonic, not phasic, measurement [Boucsein, Schaefer & Neijenhuisen, 1989]. Nevertheless, measurement methods in phasic alternating current are the more useful in testing electrical models of electrodermal response; such methods were developed for such adequate measurement concepts, for continuous recording of impedance and of angular phase, the latter seconding impedance as a descriptor of the physiological parameters [Chumlea & Guo, 1997, Baumgartner, Chumlea & Roche, 1988; Lukaski & Bolonchuk, 1987; Subramanyan, Manchanda, Nyboer & Bhatia, 1980], expressed in degrees, as an arctangent ratio  $X_c/R$ , function of current frequency used.

Branch literature also notes the existence of two distinct types *human electrical impedance* [Sutherland, Dorr & Gomatom, 2005], i.e. skin impedance, which is a surface impedance; and internal impedance, of the whole body, which is in principle resistive. The surface epidermis layer, containing both dead cells, deposited on a live layer, heterogeneous and anisotropic, illustrates both resistance and capacitance [Sălceanu, Iacobescu & Anghel, 2013]. Capacitive impedance falls in direct variance with the frequency values for high resistance.

A number of authors remark the drawbacks of the method of using alternating current in electrodermal measurements, due to the skin capacitive features, which push up conductance values [Fowles, Christie, Edelberg, Grings, Lykken & Venables, 1981].

Since, as above indicated, skin capacitance varies directly with the measuring frequency, by using under 40 Hz low frequency through a phase-sensitive rectification skin capacitance can become negligible.

By experimental results, quoted authors have proven that the electrodermal potential is a more pregnant parameter than conductance, as being much less dependent on stability of skin region contact with electrode, a fact which causes artefacts to be more pronounced in skin conductance curves, than in potential curves.

The method which Fowles used in 1981 requires direct current, and cannot tell apart conductance from the electrodermal potential waves. In order to research triggering of electrodermal mechanisms, electrodermal potential will not be measured in direct current; and will be compared with the conductance results in alternating current, which is possible by phase-sensitive adjustment, by real-time signal processing, and by variables conversion.

The measuring system in alternating current is much more complex, needing a higher number of parameters monitored; however, AC conductance allows for simultaneous measurement of

electrodermal potentials, too, in the same skin region. Also, in absence of direct current, requirements are much less restrictive for the electrode technique, no monitoring of error potentials being needed, or of polarization error during usage. Last but not least, unlike with direct current usage, sensors do not attack the skin, AC conductance bearing no influence from electric motor voltage change.

The electrodermal potential becomes thus a valuable index, enabling us to reach at the autonomic and somato-motor aspects of cognitive operation – emotion, motivation and attention; electrodermal potential manifests in absence of direct current, with the possibility to connect, by unipolar sensors usage, two aspects: *electrodermal potential level (SPL)* and *electrodermal potential response (SPR)*, such aspects being considered in model applied by present research [Grigore, 2014].

#### 4. EDA biosignals measuring procedure

##### 4.1 Phasic neurostimulation

A number of our recent studies [Grigore, 2013] note that when an alternative voltage signal is used, as well as a step signal, for simultaneous skin stimulation, in phasic state thereof the electrodermal response liability, respectively, stability level of different individuals can be easily determined. Response potential, in such case AC, acts as an *inferential marker*.

Such type stimulation opens projective psychophysical biunivocal correspondences. Electrical markers can thus fairly accurately evaluate the bioelectrical events accompanying autoregulation processes [Paraschiv, Grigore & Constantin, 2013].

A neurostimulator channel being opened sets in correspondence the region being measured with the targeted psychophysical function; whereas the neurosignals picked at sensors' level contain information regarding applied stimulus response pattern; such information must be adequately analyzed, for the mental states aspects to be extracted [Paraschiv, Grigore & Constantin, 2013].

We approached such *neurostimulation* procedure in the prospect of the implied signals mix: *step excitation* signal, *AC excitation* signal and step response signal [Grigore & Moldovan, 2015].

*Step excitation signal* (see Fig. 14, a) compounds with the sinusoidal excitation signal (see Fig. 14, b).

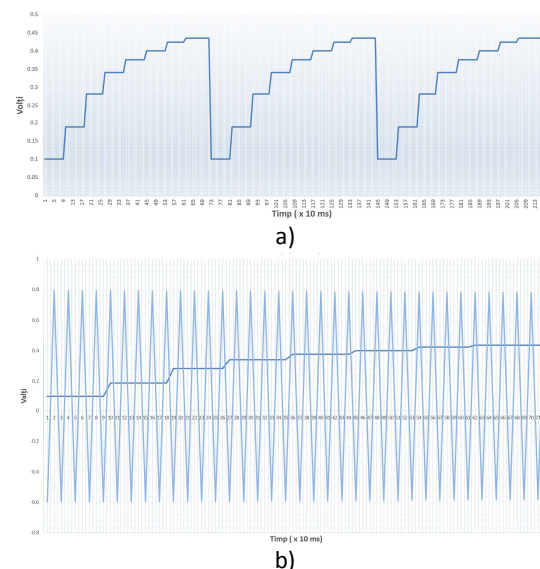


Fig. 14: Excitation signal: a) step excitation signal; b) AC excitation signal.

*Response signal*. Fig. 15 indicates the electrodermal response signal to a single excitatory impulse.

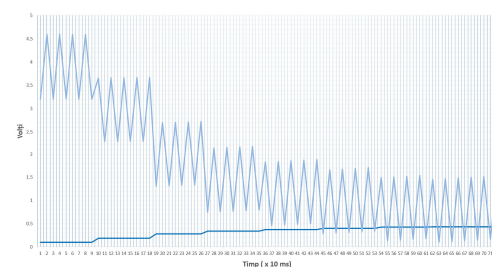


Fig. 15: Diagram illustrating step response signal in phasic neurostimulation by a single excitation impulse

Raw (acquisition) data underwent a filtering procedure, for ousting artefacts and for formatting, in view of usage thereof in inferential algorithm.

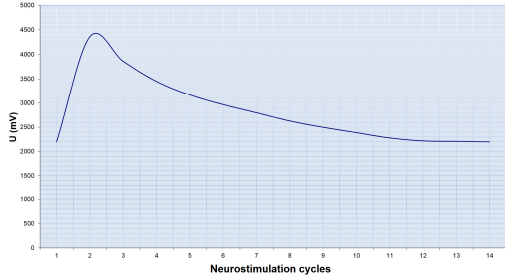


Fig. 15. AC neurostimulated skin potential response (SPR) diagram, after filtering and formatting procedure

#### 4.2 Electrodermal inferential model

*Inferential function* will act as regulation function in the electrodermal model as well (see Fig. 16).

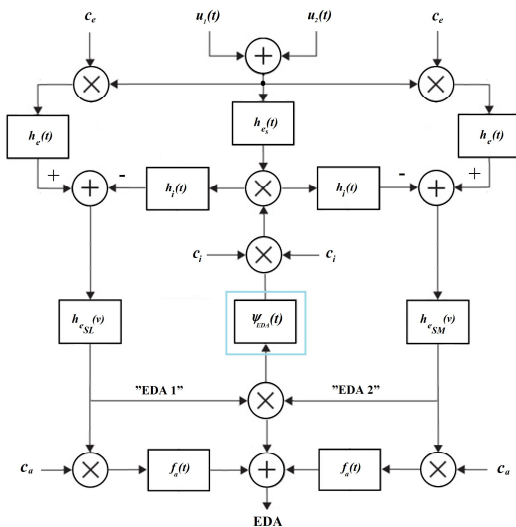


Fig. 16. Electrodermal inferential model (EIM)

Specific here are the two external stimulus signals of galvanic skin response,  $u_1(t)$  and  $u_2(t)$ , which engender an excitation function  $h_{es}(t)$ , and activation (firing) functions,  $f_a(t)$ , responsible for opening response channels, which are the expression of spontaneous stimulus sent through the activating nerve cells  $c_a$ , and manifested in *electrodermal liability*.

The *inferential electrodermal model* that we advance there exists a symmetrical linear system reacting to an excitatory impulse  $h_e(t)$ , activated by the  $c_e$  nerve cells; respectively, a similar inhibiting system manifested by functions  $h_i(t)$ , under the action of inhibitor neural cells  $c_i$ , conjugated on the

regulation loop with the *inferential function*  $\psi_{EDA}(t)$ .

The excitatory impulse, compound with the stimulation functions, will generate, at limbic system level, respectively at motor system level, the nonlinear behavior described by  $h_{e_{SL}}(v)$  and  $h_{e_{SM}}(v)$ , whose variations are projectively expressed by the *inferential function*, so that, it becomes possible to identify changes (in the basal physiological changes table) of muscular tonus intensity and distribution, of skin electrical resistance and conductivity (e.g. fear and fright drop, self-possessiveness and good temper increase), and such like.

Fig. 17.A illustrates a quite simplified electrical diagram of the electrodermal inferential model (EIM).

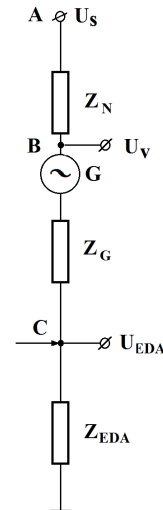


Fig. 17. Simplified EIM electrical diagram

In terms of electricity, after firing the electrodermal chain by activation of impedance  $Z_{EDA}$ , source  $G$  of  $Z_G$  impedance opens and becomes active, such activity being described by the inferential function  $\psi_{EDA}(t)$ . Source activation is possible by applying the excitation signal at point C level. The real form of a firing signal manifested by activation of impedance  $Z_{EDA}$  is illustrated in Fig. 18, where, for the seven stimulation channels, the firing sessions will be noted only for the first step impulse, respectively for the last two.

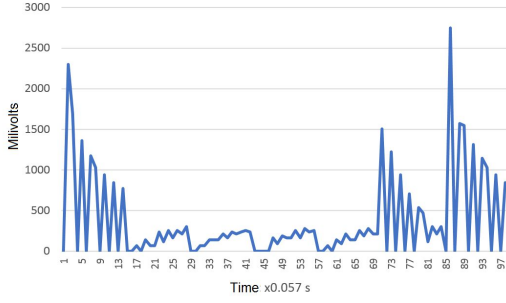


Fig. 18. Skin impedance firing real signal

Actual voltages balance at point B level can be expressed as  $U_V = U_G + U_{EDA}$ , a sum expressible function of the two impedances and actual current running through, as stated below:

$$U_V = I(Z_G + Z_{EDA}) \quad (22)$$

Balance (22) for a relatively low time value, will meet requirement below:

$$Z_G + Z_{EDA} = ct. \quad (23)$$

Condition (23) states the relation of the two impedances, respectively the work regime of source G, of interest for present study. Hence the following relations:

$$\begin{aligned} Z_G \uparrow &\Rightarrow U_G \uparrow \\ Z_{EDA} \downarrow &\Rightarrow U_{EDA} \downarrow \end{aligned} \quad (24)$$

Such relations illustrate the direction of source G activation or inhibition, visible through level  $U_{EDA}$ , as measured in point C. In other words, when skin conductance rises, source G is active, function  $\psi_{EDA}(t)$  describing linear activity thereof.

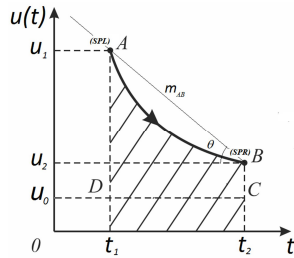


Fig. 19. Graph for a transit model of an AC electrodermal neurostimulated potential.

In order to determine the mathematical expression of the AC neurostimulated electrodermal potential dynamics, ultimately expressed as an inferential function, we applied graph in Fig. 19, where transition function  $u(t)$  was evaluated, from point A

where *skin potential level (SPL)* value is acquired; to point B, where the *skin potential response (SPR)*, is acquired [Grigore, 2016].

#### 4.2.1 Allotted energy

AC galvanic skin neurostimulation process runs simultaneously, for the same subject, along a number of channels. The effect that such stimulation can possibly cause, reflected by electrodermal potential transition, is evaluated as power. For each stimulated *ichannel*, allotted power form will be:

$$P_i(t) = I_i \cdot u_i(t) \quad (25)$$

where  $I_i$  is taken to be stable (stability granted through neurostimulation equipment development), so that energy consumed in transit can be determined by integrating relation (25):

$$S_i(t) = I_i \int_{t_1}^{t_2} u_i(t) dt \quad (26)$$

$S_i$  expressing *energy allotted* to channel  $i$  in neurostimulation. For the whole process, on  $i$  stimulation channels  $i$ ,  $(\forall) i = \overline{1, n}$ , allotted energy is expressed as a matrix, as further detailed:

$$S = \begin{pmatrix} S_1(t) \\ S_2(t) \\ \cdot \\ \cdot \\ S_i(t) \end{pmatrix} \quad (27)$$

#### 4.2.2 EDA inference Level

We took each neurostimulation source afferent to a channel  $i$  to manifest an inference specific to a bandwidth  $j$ ,  $(\forall) j = \overline{1, n}$ .

That is why we studied how allotted energy  $S_i$  manifested in physiological potential  $\varphi$ , produces *inference*  $\gamma$  on a paired measuring channel  $i$  and bandwidth  $j$ . Relation of  $\varphi$  and  $\gamma$  is as further detailed:

$$\gamma = \beta \cdot \varphi \quad (28)$$

where  $\beta$  is a scale factor, form  $\tau/(u_{max}-u_0)$ ,  $u_{max}$  is maximum potential on scale used, whereas  $u_0$  is the response potential minimum value, up to which a psychophysical inference can be intercepted [Grigore, 2016].

The characteristic transition neurostimulation index, an AC electrodermal potential, is parameter  $m_{AB}$ ,

defined as the slope of the line containing segment AB (see Fig. 19). The form of  $m_{AB}$ , for a neurostimulation channel  $i$ , can be expressed as below:

$$m_{AB_i} = \frac{u_{1i} - u_{2i}}{|t_1 - t_2|} \quad (29)$$

Significance of slope  $m_{AB_i}$  depends on by skin potential response (SPR) level, position thereof being a function which varies directly with the psychophysical *inference level*. Parameter variation  $m_{AB_i}$  may be seen for  $u_{1i} = u_{2i}$ , where  $m_{AB_{MIN}} = 0$ ; respectively for  $u_{2i} = u_0$ , there resulting a relation as further expressed:

$$m_{AB_{MAX}} = \frac{u_{1i} - u_0}{|t_1 - t_2|} \quad (30)$$

Given that each transition along a channel  $i$  produces a specific inference on a bandwidth  $j$ , form of slope  $m_{AB_j}$  afferent to bandwidth  $j$ , for a minimum  $u_0$  potential value, can be expressed as:

$$m_{AB_j} = \frac{u_{1j} - u_0}{|t_1 - t_2|} \quad (31)$$

We will define physiological component  $\Phi_{ij}$  in inferential relation, for channel  $i$  and bandwidth  $j$ , as potential SPR measured on *stimulation channel* multiplied by ratio of slope afferent to *stimulation channel* and slope of *inference bandwidth*, as further expressed:

$$\phi_{ij}(u) = u_{1i} \frac{m_{AB_j}}{m_{AB_i}} \quad (32)$$

relation by means of which, *inference* form (28) becomes:

$$\gamma_{EDA_{ij}} = \frac{u_{1i}(u_{1j} - u_0)}{(u_{\max} - u_0)(u_{1i} - u_{2i})} \quad (33)$$

In order to determine *inferential electrodermal function*  $\Psi_{EDA_{ij}}$  form, we considered electrodermal potential transit for a channel  $i$ ; also, the way in which transit causes inferencese, and the mean electrodermal potential response, at level of all  $i$  neurostimulation channels. We defined efficiency of neurostimulation process along channel  $i$ , as the ratio of energy allotted to such channel  $i$  and the

mean of the energies allotted on all of the channels [Grigore, 2016].

By means of the relation (26) we set the form of the mean energy allotted by neurostimulation to all of the channels  $i$ :

$$\bar{S} = \frac{I}{i} \int_{t_1}^{t_2} (u_1(t) + u_2(t) + \dots + u_i(t)) dt \quad (34)$$

where we considered  $I_1 = I_2 = \dots = I_i = I$ , a requirement granted by the neurostimulation equipment construction.

(26) and (34) yield efficiency for each channel  $i$  as further expressed:

$$\begin{aligned} \rho_{EDA_i} &= \frac{I \int_{t_1}^{t_2} u_i(t) dt}{I \int_{t_1}^{t_2} (u_1(t) + u_2(t) + \dots + u_i(t)) dt} \\ &= i \frac{\int_{t_1}^{t_2} u_i(t) dt}{\int_{t_1}^{t_2} (u_1(t) + u_2(t) + \dots + u_i(t)) dt} \end{aligned} \quad (35)$$

On the other hand, considering that the psychophysical inference ratio implies the inferential reproduction of the whole psychological functions  $\Psi_{EDA_{ij}}$  table, we determined that, for development thereof, inferential relation of factors will be expressed as:

$$\Psi_{EDA_{ij}} = \rho_{EDA_i} \gamma_{EDA_{ij}} \quad (36)$$

signifying *electrodermal inferential indices*, components which, considering (33), yielded the final form of *electrodermal psychophysical tensor*  $\Psi_{EDA_{ij}}$ :

$$\Psi_{EDA_{ij}} = \frac{\tau}{u_{\max} - u_0} \begin{pmatrix} \rho_1 u_{11} \frac{u_{11} - u_0}{u_{11} - u_{21}} & \rho_1 u_{11} \frac{u_{12} - u_0}{u_{11} - u_{21}} & \dots & \rho_1 u_{11} \frac{u_{1j} - u_0}{u_{11} - u_{21}} \\ \rho_2 u_{12} \frac{u_{11} - u_0}{u_{12} - u_{22}} & \rho_2 u_{12} \frac{u_{12} - u_0}{u_{12} - u_{22}} & \dots & \rho_2 u_{12} \frac{u_{1j} - u_0}{u_{12} - u_{22}} \\ \vdots & \vdots & \ddots & \vdots \\ \rho_i u_{1i} \frac{u_{11} - u_0}{u_{1i} - u_{2i}} & \rho_i u_{1i} \frac{u_{12} - u_0}{u_{1i} - u_{2i}} & \dots & \rho_i u_{1i} \frac{u_{1j} - u_0}{u_{1i} - u_{2i}} \end{pmatrix} \quad (37)$$

in which we identified and rewrote inferential *electrodermal index*  $\Psi_{EDA_{ij}}$  form, as:

$$\Psi_{EDA_{ij}} = \frac{u_{1i} \tau}{u_{\max} - u_0} \frac{u_{1j} - u_0}{u_{1i} - u_{2i}} \frac{\int_{t_1}^{t_2} u_i(t) dt}{\int_{t_1}^{t_2} (u_1(t) + u_2(t) + \dots + u_i(t)) dt} \quad (38)$$

**Example 3.**

We further present a computation instance, of an *electrodermal inferential index*, value, out of SPL and SPR electrodermal potentials values, for an inferential psychophysical system, size  $i \times j$ , where  $i = 7$  and  $j = 4$ :

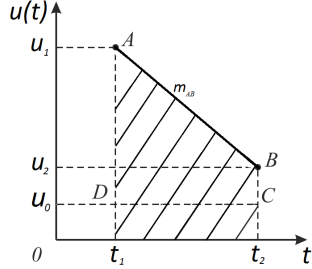


Fig. 20. Transit curve approximation

$\rho_1, \rho_2, \dots, \rho_7$  efficiencies were determined by approximation of the transition curve (see Fig. 20) to line segment  $\overline{AB}$ , rewriting the allotted energy form in such transition:

$$S_i = \frac{I}{2}(u_{1i} + u_{2i})(t_2 - t_1) \quad (39)$$

and the mean energy allotted for all of the  $i = 7$  neurostimulation channels:

$$\bar{S} = \frac{I}{14}(t_2 - t_1) \sum_{i=1}^7 (u_{1i} + u_{2i}) \quad (40)$$

(39) and (40) considered, (35) for channel  $i$ , becomes:

$$\rho_{EDA_i} = 7 \frac{u_{1i} + u_{2i}}{\sum_{i=1}^7 (u_{1i} + u_{2i})} \quad (41)$$

By substituting form (38) in (34), *electrodermal psychophysical tensor*  $\Psi$ , for size  $7 \times 4$  becomes:

$$\Psi_{74} = \frac{\tau}{u_{\max} - u_0} \begin{pmatrix} \rho_1 u_{11} \frac{u_{11} - u_0}{u_{11} - u_{21}} & \rho_1 u_{11} \frac{u_{12} - u_0}{u_{11} - u_{21}} & \dots & \rho_1 u_{11} \frac{u_{14} - u_0}{u_{11} - u_{21}} \\ \rho_2 u_{12} \frac{u_{11} - u_0}{u_{12} - u_{22}} & \rho_2 u_{12} \frac{u_{12} - u_0}{u_{12} - u_{22}} & \dots & \rho_2 u_{12} \frac{u_{14} - u_0}{u_{12} - u_{22}} \\ \dots & \dots & \dots & \dots \\ \rho_7 u_{17} \frac{u_{11} - u_0}{u_{17} - u_{27}} & \rho_7 u_{17} \frac{u_{12} - u_0}{u_{17} - u_{27}} & \dots & \rho_7 u_{17} \frac{u_{14} - u_0}{u_{17} - u_{27}} \end{pmatrix} \quad (42)$$

The electrodermal inferential functions values were determined by relation (42) for  $\tau=10$  and  $u_{\max} = 5000$  mV; and recorded on a 75 to 265 standard inferential units [u.inf.] scale.

Table 3 indicates the experiment values.

Table 3. Experiment values

| Nr. canal | SPL             | [mV] | SPR             | [mV] | $\rho$ | $\Psi_{i1}$ [u.inf.] | $\Psi_{i2}$ [u.inf.] | $\Psi_{i3}$ [u.inf.] | $\Psi_{i4}$ [u.inf.] |
|-----------|-----------------|------|-----------------|------|--------|----------------------|----------------------|----------------------|----------------------|
| 1         | U <sub>11</sub> | 4750 | U <sub>21</sub> | 4450 | 1.11   | 165.34               | 124.56               | 143.96               | 148.06               |
| 2         | U <sub>12</sub> | 3925 | U <sub>22</sub> | 3710 | 0.92   | 158.21               | 119.19               | 137.75               | 141.67               |
| 3         | U <sub>13</sub> | 4265 | U <sub>23</sub> | 4004 | 1.00   | 153.38               | 115.54               | 133.54               | 137.34               |
| 4         | U <sub>14</sub> | 4358 | U <sub>24</sub> | 4150 | 1.03   | 202.34               | 152.43               | 176.17               | 181.19               |
| 5         | U <sub>15</sub> | 4650 | U <sub>25</sub> | 4456 | 1.10   | 247.75               | 186.64               | 215.70               | 221.85               |
| 6         | U <sub>16</sub> | 4035 | U <sub>26</sub> | 3856 | 0.96   | 201.91               | 152.10               | 175.79               | 180.80               |
| 7         | U <sub>17</sub> | 3789 | U <sub>27</sub> | 3502 | 0.88   | 109.26               | 82.31                | 95.13                | 97.84                |

**4.2.3 EDA biosignals acquisition. MindMi™ psychological evaluation system**

MindMi™ Integrated System implements a neurostimulation procedure, respectively the inferential model above described. Equipment for the acquisition of stimulated electrodermal response potentials is the palm scanner MindSpring™, (see Fig. 21), an electronic equipment expressing the updated variant, with facilities for cloud computing, patented by author as *Electronic Equipment and Fast Evaluation Method of Psychological Profiles - RO127615*, [Grigore, 2013].

Such equipment generates, formats and applies step voltage signals, and sinusoidal signals on measuring regions of the palm, through silver type sensors adequately located on upper side of such electronic equipment lid, stimulation the skin in alternating current.



Figura 21: MindMi™ Psychometric System (<https://www.mindmismystem.com>)

Scanning equipment can measure electrodermal parameters in a very low scanning time, being able to reach a server by any device and computation means, to connect to internet by desktop, laptop, iPod, cell phone, and such like.

Being run in a computation equipment configuration, endowed with integrated mini-computer (a solution conferring autonomy) equipment can be used for running scanings even in case the internet connection falls, data scanned being checked, validated, pre-processed, saved and readied to be sent to server after reconnection online.

By such capacity for processing, checking and validation acquisition data in real time, at scanning equipment level, equipment supplies the user the

variability analysis rate of the acquired signal level, so that, for a low enough variation of the whole signals set, the scanning session being possibly stopped before maximum time limit allotted to reading cycles, a fact which causes a high data validation and fidelity.

The scanner takes over electrodermal information with a low work frequency, thus barring out any interference with any proximal source of radioelectrical signal. By means of the implemented software program, the scanner records the SPR AC-stimulated response potentials over a specific number of measuring cycles, also reading and storing such signals' amplitude values [Grigore, R2, 2015].

Method uses a solution type cloud computing by galvanic neurostimulation of the skin and, consequently, as per autoregulation principle, by inverse connection installed between system outlets and input sensors region, phasic conductance response perceived by skin will be in projective correspondence with the bioelectric events occurred

## 5. Cognitive typology weighing

### 5.1 EEG-EDA inferential dual module

Dual behavior analysis of electroencephalographic and electrodermal response biosignals can start from local model (LEM) advanced by [Wilson & Cowan, 1972] where, as indicated (at 2.4.2; see Fig. 9), we take the regulation function to be inferential. In the branch of the neural processes resulting in AC stimulated electrodermal response, model (MIE) advanced also uses such electrodermal inferential function as a regulation function.

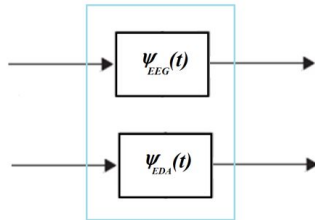


Fig. 21. Inferential dual module

Fig. 21 presents a dual inferential module which we considered in present study and based on which we advanced unified concept EEG-EDA, which yield factual experimental results, in the behavioral aspects. In order to cover targets advanced, we identified a common form for the cognitive psychological aspects under consideration.

#### 5.1.1 Cognitive function

Aspects of interest as determining cognitive typologies correlate with the specific way in which inferential indices find an expression in cognitive

in organism, generated during the autoregulation processes by which psychophysical functions are manifested.

Opening a neurostimulator channel will set in correspondence the measuring region with the targeted psychophysical function, whereas the neurosignals picked at sensors level will contain information regarding the response pattern for the stimulus applied. Such aspect manifests through actual projective probing of the brain waves, in view of identification one set of variables which, correlatively interpreted, will supply an objective psychological profile to the individual evaluated.

A number of interrogations of the measuring regions will be run, by applying at skin level one step excitation signal and a carrier sinusoidal signal, recording and stocking simultaneous response signals, skin conductance variations, expressed in corresponding to voltage variations, over each interrogation cycle, together with excitation signal, in a file of ratio-input data.

acts. The table of inferential indices can be expressed by a set of cognitive functions, as indicated below:

$$C = \alpha \cdot \psi \quad (43)$$

where  $\alpha$  expresses *inferential weigh*, measuring the manifesting level of the inferential index in cognitive function. Cognitive function tensor is expressed as weightings matrix multiplied by the inferential indices, as below:

$$C_{ij} = \begin{pmatrix} \alpha_{11} & \alpha_{12} & \dots & \alpha_{1i} \\ \alpha_{21} & \alpha_{22} & \dots & \alpha_{2i} \\ \dots & \dots & \dots & \dots \\ \alpha_{k1} & \alpha_{k2} & \dots & \alpha_{ki} \end{pmatrix} \cdot \begin{pmatrix} \psi_{11} & \psi_{12} & \dots & \psi_{1j} \\ \psi_{21} & \psi_{22} & \dots & \psi_{2j} \\ \dots & \dots & \dots & \dots \\ \psi_{i1} & \psi_{i2} & \dots & \psi_{ij} \end{pmatrix} \quad (44)$$

which becomes as further expressed:

$$C_{ij} = \sum_{k=1}^n \alpha_{ki} \psi_{kj}, (\forall) k = \overline{1, n}; (\forall) j = \overline{1, n} \quad (45)$$

#### 5.1.2 Inferential pattern, cognitive typology

In order to identify the cognitive typologies, matrix  $C_{ij}$  factors will be paired based on a number  $m$  of polarity criterions, thus yielding a set of inferential pattern, expressible as below:

$$S_{pq} = \left[ \left( \sum_{i=1}^n \alpha_{ki} \psi_{ij} \right)_p \left( \sum_{i=1}^n \alpha_{ki} \psi_{ij} \right)_q \right], (\forall) p = \overline{1, m}; (\forall) q = \overline{1, m} \quad (46)$$

Compounding the inferential patterns can yield a number  $t = m(m-1)$  of cognitive typologies, expressible as:

$$V_{xy} = \left( S_{pq} \right)_x + \left( S_{pq} \right)_y, (\forall) x = \overline{1, t}; (\forall) y = \overline{1, t} \quad (47)$$

which, in their turn, pair into  $m$  cognitive classes. By selecting the weighing the highest value in sum (47), the most stable cognitive typology was begot. [Grigore, 2016]

### 5.1.3 Weighing correspondences of EEG-EDA cognitive typologies biunivocal relations

In multiple experiments, on an number of subjects simultaneously evaluated by means of MindMi™ System and NeuroSky headset, and by application of mediation on *power spectral distribution* on each bandwidth in view of determining the inferential functions, respectively the EEG cognitive functions, we found a persistent occurrence of a specific pattern whose low variability is of interest for our comparative study, electrodermal response of which being yielded by galvanic neurostimulation procedure.

In our approach we targeted interception of the most stable cerebral behavior. Our vision aims to identify the specific factors and features of the stable behavior types, which will finally yield indices related to personality typologies expressed in both EEG, and EDA, phenomenology.

The dual experiment we ran on EEG, respectively EDA, biosignals, correlated two brain frequency bandwidth regions within which is the two types *cognitive functions* manifest. In order to distinguish between the afferent functions of such two regions, we took such *cognitive functions* to be *tonic*, respectively *atonic*. Considering such functions based on brain frequency bandwidth highlights a series of *high* and *very high frequency* (tonic) cognitive functions, respectively a distinct series of *low* and *quite low frequency* (atonic) cognitive functions (see Table 4).

Identification of EEG-EDA functions pairs require a ranking routine based on correlation level between such functions groups, evaluated progressively, up to *one-to-one* functional identification. Fig. 23 below instances a diagram of patterns made of EEG and EDA cognitive functions pairs, identified by a progressive sorting out routine.

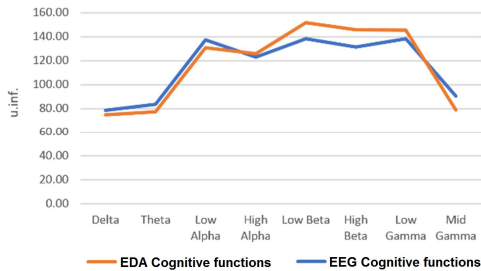


Fig. 23. Progressive EEG and EDA cognitive functions pattern, as yielded by simultaneous acquisition data

In order to assess cognitive typologies for a lot of subjects evaluated simultaneously by EEG and EDA measuring devices, a *weighing function* must be determined, equally expressed in cognitive components measurable by electroencephalography and electrodermally. *Weighing function*, mediated at lot level, expresses intelligibly level of a cognitive typology, as determined by EEG-EDA measuring.

Table 4: Ranking cognitive functions based on brain frequency bandwidth

|                            |   |            |
|----------------------------|---|------------|
| Tonic cognitive functions  | Very high frequency cognitive functions | Mid Gamma  |
|                            |   | Low Gamma  |
|                            | High frequency cognitive functions      | High Beta  |
|                            |   | Low Beta   |
| Atonic cognitive functions | Low frequency cognitive functions       | High Alpha |
|                            |   | Low Alpha  |
|                            | Very low frequency cognitive functions  | Theta      |
|                            |   | Delta      |

For a start, we state that  $C_{TONi}$  is a tonic cognitive function, while  $C_{ATONi}$  is an atonic cognitive function. For a pair of complementary cognitive functions, there is a *behavior function*  $K_i$ , whose form is expressible as below:

$$K_i \Big|_{EEG;EDA} = \begin{cases} A_i; C_{TONi} > C_{ATONi} \Big|_{EEG;EDA} \\ B_i; C_{TONi} \leq C_{ATONi} \Big|_{EEG;EDA} \end{cases} \quad (48)$$

Behavior function will thus be found in cognitive typology, expressible as below:

$$V \Big|_{EEG;EDA} = (K_1; K_2; \dots; K_n) \Big|_{EEG;EDA} \quad (49)$$

whereas in order to compare manifest expression of a cognitive typology in biosignals distinct in terms of physiology, *weighing function* afferent to behavior  $K_i$  is expressible as below:

$$h_i \Big|_{EEG;EDA} = \begin{cases} h_{\max}; K_i \Big|_{EEG} = K_i \Big|_{EDA}; (\forall) i = \overline{1, n} \\ 0; K_i \Big|_{EEG} \neq K_i \Big|_{EDA} \end{cases} \quad (50)$$

where  $h_{\max} = \frac{100}{2n}$ .

Based on (50) total weighing function for one subject in the lot is expressible as below:

$$H|_{EEG;EDA} = \sum_{i=1}^n h_i|_{EEG;EDA} \quad (51)$$

respectively the mean weigh, for a lot of  $m$  subjects is expressible as below:

$$\bar{H}_m|_{EEG;EDA} = \frac{1}{m} \sum_{j=1}^m \sum_{i=1}^n h_{ij}|_{EEG;EDA} \quad (52)$$

#### 5.1.4 Correlation of EEG-EDA cognitive function probability values

Let  $S$  be a space whose subassemblies consist in the sum total of behavior functions  $K_i$  taken as additive classes, made of events whose values are  $A_i$  and  $B_i$ , as per (48). To each event  $k$  in class  $K_i$  corresponds

## 6. The coordinates of the experimental work

### 6.1. Introduction

The experimental work uses an original method ensuring a double interception of the brain activity, so as to determine the relation between electroencephalographic and electrodermal potentials, inferentially expressed in personality typologies. The double interception of the brain activity is expressed in the correlation between the *cognitive functions*, as determined from the average of the *power spectral densities* of the EEG biosignals and those determined from the basal electrodermal (SPL) and response (SPR) potentials, according to the explanations from 5.1. The research therefore refers to the use of two different techniques, which involve biosignals of different physiologies, in order to obtain appropriate variables for every technique in part, the same type of cognitive behaviour, expressed in electrical signal.

### 6.2. Assumption

It is known that the electrodermal response in conductance is the effect of the activity of the sweat glands. When they have an abundant secretion, phasic changes appear by increasing the conductance, i.e. when the moisture gets absorbed, the conductance comes back to the basic values. The behaviour of the sweat glands, to this respect, may be compared to some resistances of which values, reverse from the conductance, decrease when moisture is maximum and increase when it drops to normal value, the amount of fluid secreted by the glands and their number, simultaneously evaluated, being inversely related to the amplitude of the conductance changes [Edelberg, 1968; Boucsein, 2012].

Also, the process of stimulating the phasic electrodermal level, with a stepped and a sinusoidal signal, may show response potentials connected to autonomous and somatic-motor aspects of the cognitive function. [Grigore, 2014].

a real number  $0 \leq P(k) \leq 1$  will correspond, named *k probability*, a *sure event*  $s$  being expressible as  $P(s) = 1$  (as per Kolmogorov's axioms). For a lot of  $m$  subjects, prone to  $n$  behavior functions, cognitive functions probabilities  $P_m(k_1); P_m(k_2); \dots; P_m(k_n)$  will be expressible as below:

$$\frac{2}{n} \sum_{i=1}^n P_m(k_i) = 1 \quad (53)$$

The strings of probabilities  $P_m(k_i)|_{EEG}$ , respectively  $P_m(k_i)|_{EDA}$ , can be analyzed statistically.

Based on these considerations, we assume that there is a significant correlation between the values of the *cognitive functions* determined by the average of the *spectral power densities of the EEG biosignals* taken from the scalp and the *cognitive functions* corresponding to the basal (SPL) and response (SPR) electrodermal potential measured at the same time, on the palms of the same individual.

### 6.3 Method, electronic equipment, measurement and analysis software, participants

The tests were conducted on a sample of 100 subjects aged between 20 and 65 years. The participation in the experiment was by voluntary option, each of the subjects being informed on the conditions of the experiment.

For the performance of the experimental work, we used as *electrodermal neurostimulator*, the palm scanner of the psychometric system MindMi™ presented in 4.2.3, by means of which we applied, on the palms of the evaluated subject, an electrodermal excitation signal, obtained by composing two signals: one step signal and one bearing signal, and we received through the specialised acquisition interface a response signal of which envelope contains essential information about the psychophysiological processes on which we proposed to identify an inference. Hence, we expressed the projective response of the neurocortex, on each channel in part, in inferential functions, determined by information about the level of electrodermal activity, by identifying the levels of electrodermal potential, stimulated in alternative current of SPL type - basal potential and SPR type - response potential. Also, we made a simultaneous take-over, through an acquisition server interface, model Open VIBE v1.2.2, from the INRIA, of a set of EEG-type signals from the forehead of the same individual, by means of the professional headpiece Neuro Sky MindSet (Figure 24).

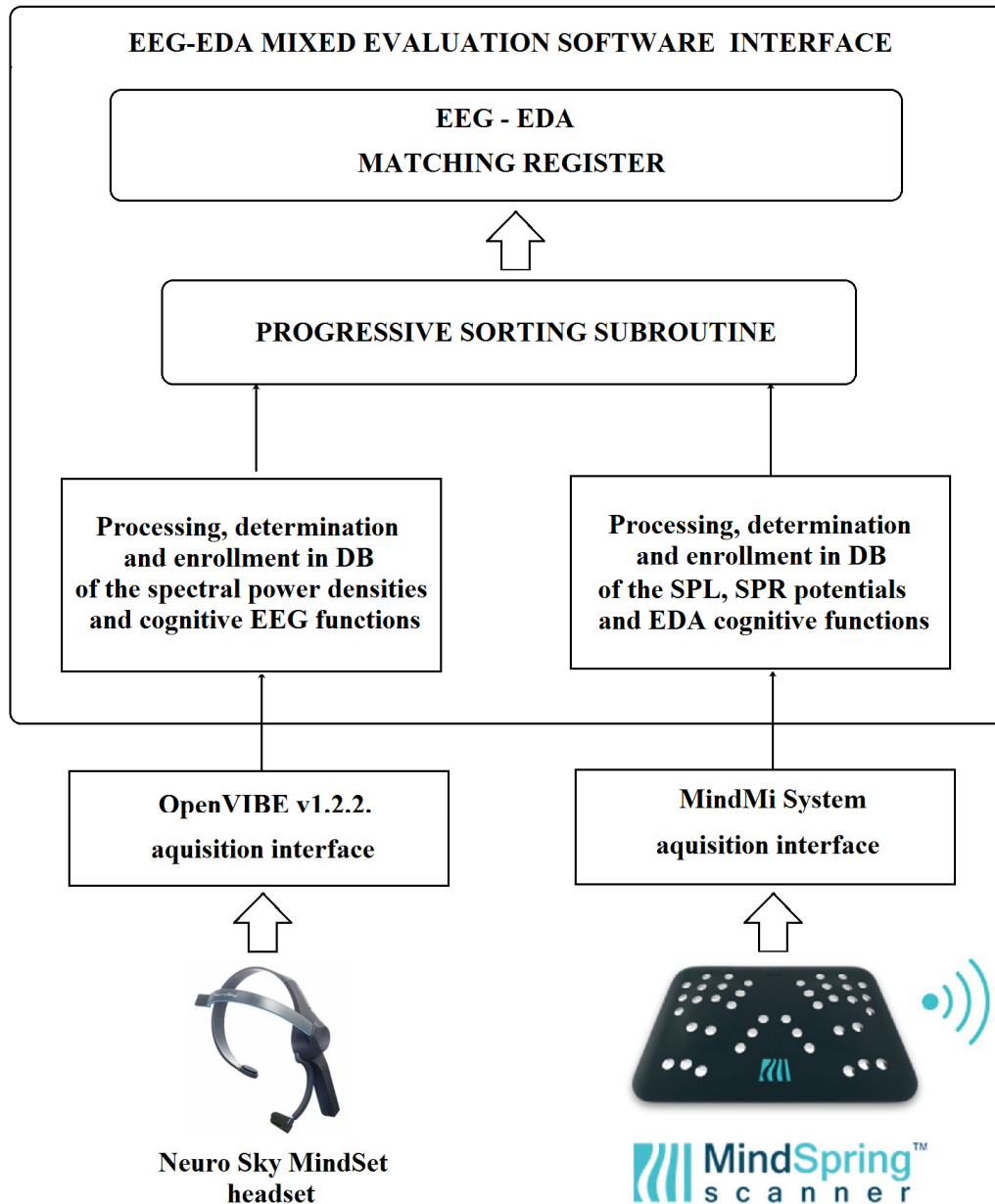


Figure 24: Flow chart of the measurement system

**Progressive sorting of the pair functions.** With the purpose to determine the cognitive typologies for  $m = 4$  polarity criteria (cognitive classes), both EDA biosignals and EEG biosignals have been processed with an original software interface, particularly designed for this experiment, for the results to be subject to a correlation analysis. The software interface uses the mathematical model presented in 2.4.2, 4.2 and 5.1. with the purpose to identify and store mixed cognitive functions, as also the progressive sorting subroutine (Figure 25), by means of which a one-on-one correspondence between them is identified for Pearson bivariate correlation assays made on the sample of 100 subjects.

After completing the database enrolment process, the set of EEG cognitive functions ( $F_1, F_2, F_3, F_4, F_5, F_6, F_7$  and  $F_8$ ) related to the brain frequency bands is established. These functions, grouped based on the criteria provided in Table 4, are reference to progressive sorting. The result of this multistage selection of the EDA function, corresponding to an EEG, is included in a pair record. The *tonic* and *atonic* cognitive functions so determined are established in bipolar indicators of inferential pattern. The correspondence from the pairs record is presented in Table 5.

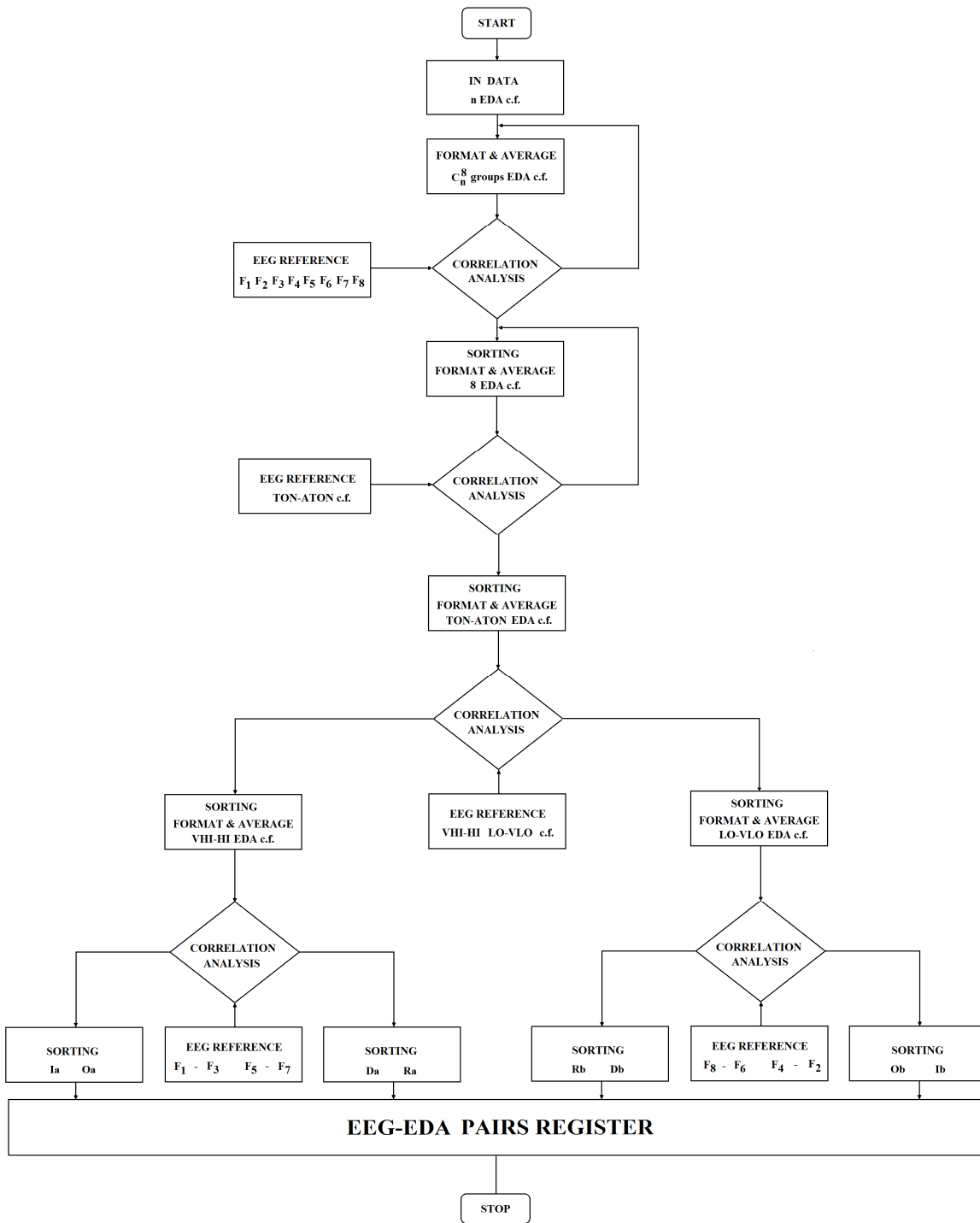


Figure 25: The algorithm of progressive sorting subroutine

Table 5: The correspondence between *tonic* and *atonic* cognitive functions in brain frequency bands

| EDA<br>COGNITIVE FUNCTIONS |         |    | FREQUENCY<br>BANDS | EEG<br>COGNITIVE FUNCTIONS |         |          |
|----------------------------|---------|----|--------------------|----------------------------|---------|----------|
| TON_EDA                    | VHI_EDA | Ia | Mid Gamma          | F1                         | VHI_EEG | TON_EEG  |
|                            |         | Oa | Low Gamma          | F3                         |         |          |
|                            | HI_EDA  | Da | High Beta          | F5                         | HI_EEG  |          |
|                            |         | Ra | Low Beta           | F7                         |         |          |
| ATON_EDA                   | LO_EDA  | Rb | High Alpha         | F8                         | LO_EEG  | ATON_EEG |
|                            |         | Db | Low Alpha          | F6                         |         |          |
|                            | VLO_EDA | Ob | Theta              | F4                         | VLO_EEG |          |
|                            |         | Ib | Delta              | F2                         |         |          |

**Establishing the cognitive typologies.** After determining the inferential pattern bipolar indicators: Ia, Ib, Oa, Ob, Da, Db, Ra și Rb and their related values, four sets of indicators have been extracted, corresponding to the behavioural functions  $K_i$ ,  $K_o$ ,  $K_D$ , și  $K_R$  of which meaning was assigned in a bipolar manner according to the formula (48), thus  $K_i$  received one of the values  $Ia$  and  $Ib$ ,  $K_o$  received one of the values  $Oa$  and  $Ob$ ,  $K_D$  received one of the values  $Da$  and  $Db$ , and  $K_R$  received one of the values  $Ra$  and  $Rb$ .

In order to establish the cognitive typology, formula (47) was used to calculate the shares resulted from summing up the values of the cognitive functions, organising each set of indicators corresponding to the functions  $K_i$ ,  $K_o$ ,  $K_D$ , și  $K_R$  in two groups of indicators with an antagonistic inferential significance. The value of a bipolar indicator is given by the arithmetic average of the values of the indicators corresponding to a group. By comparing the values of the pair of inferential pattern bipolar indicators, the highest value was selected, which constitutes the share of the set of indicators corresponding to each behavioural function  $K$ . The inferential patterns  $S1...S8$  were assigned to the cognitive typologies  $V$ , so each typology will have a corresponding number of two patterns and each pattern will have two bipolar indicators out of the eight. The relation between the cognitive functions ( $C_i$ ) that meet here the role of bipolar indicators, the inferential patterns ( $S_{pq}$ ), the cognitive

typologies ( $V_{xy}$ ) and the cognitive classes ( $T_m$ ) is presented in Table 6.

Table 6: Assigning the inferential patterns in cognitive typologies

|    |         |         |         |         |     |    |    |
|----|---------|---------|---------|---------|-----|----|----|
| T1 | S2      | S6      | S1      | S3      |     |    |    |
|    | Db   Rb | Da   Rb | Oa   Ib | Ib   Ob | V1  | S2 | S1 |
|    |         |         |         |         | V2  | S2 | S3 |
|    |         |         |         |         | V5  | S6 | S1 |
|    |         |         |         |         | V6  | S6 | S3 |
| T2 | S2      | S6      | S4      | S5      |     |    |    |
|    | Db   Rb | Da   Rb | Ia   Oa | Ia   Ob | V3  | S2 | S4 |
|    |         |         |         |         | V4  | S2 | S5 |
|    |         |         |         |         | V7  | S6 | S4 |
|    |         |         |         |         | V8  | S6 | S5 |
| T3 | S1      | S7      | S8      | S3      |     |    |    |
|    | Oa   Ib | Ra   Db | Da   Ra | Ib   Ob | V9  | S7 | S1 |
|    |         |         |         |         | V10 | S7 | S3 |
|    |         |         |         |         | V13 | S8 | S1 |
|    |         |         |         |         | V14 | S8 | S3 |
| T4 | S4      | S7      | S8      | S5      |     |    |    |
|    | Ia   Oa | Ra   Db | Da   Ra | Ia   Ob | V11 | S7 | S4 |
|    |         |         |         |         | V12 | S7 | S5 |
|    |         |         |         |         | V15 | S8 | S4 |
|    |         |         |         |         | V16 | S8 | S5 |

To determine the cognitive typology, we evaluated a group of 16 shares  $Pv1, Pv2, \dots, Pv16$ , corresponding to the 16 typologies. The evaluation of these shares is made by comparing the related sums calculated from the values of the bipolar indicators of inferential pattern, identified as per Table 7. The highest share of these sums indicates the basic cognitive typology of the evaluated individual [Grigore, 2013].

Table 7: Assigning the bipolar indicators in shares

| Weight           | Bipolar indicators of inferential patterns |    |    |    |
|------------------|--|----|----|----|
| Pv <sub>1</sub>  | Db   | Rb | Oa | Ib |
| Pv <sub>2</sub>  | Db   | Rb | Ib | Ob |
| Pv <sub>5</sub>  | Da   | Rb | Oa | Ib |
| Pv <sub>6</sub>  | Da   | Rb | Ib | Ob |
| Pv <sub>3</sub>  | Db   | Rb | Ia | Oa |
| Pv <sub>4</sub>  | Db   | Rb | Ia | Ob |
| Pv <sub>7</sub>  | Da   | Rb | Ia | Oa |
| Pv <sub>8</sub>  | Da   | Rb | Ia | Ob |
| Pv <sub>9</sub>  | Ra   | Db | Oa | Ib |
| Pv <sub>10</sub> | Ra   | Db | Ib | Ob |
| Pv <sub>13</sub> | Da   | Ra | Oa | Ib |
| Pv <sub>14</sub> | Da   | Ra | Ib | Ob |
| Pv <sub>11</sub> | Ra   | Db | Ia | Oa |
| Pv <sub>12</sub> | Ra   | Db | Ia | Ob |
| Pv <sub>15</sub> | Da   | Ra | Ia | Oa |
| Pv <sub>16</sub> | Da   | Ra | Ia | Ob |

Fig. 26 shows an example of distribution of the specific items of the cognitive typologies for four cognitive classes.

Another form of representing the relation between the behavioural functions, the cognitive typologies

and the cognitive classes, in the design of the mixed EEG-EDA approach, is given as example in figure 27.

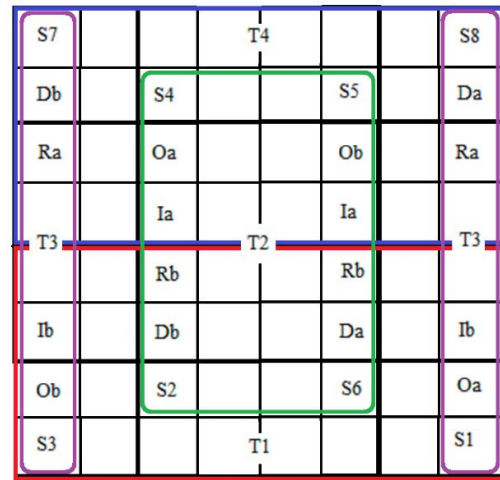


Figure 26: The distribution of specific items of the cognitive typologies for four cognitive classes [Grigore, 2016].

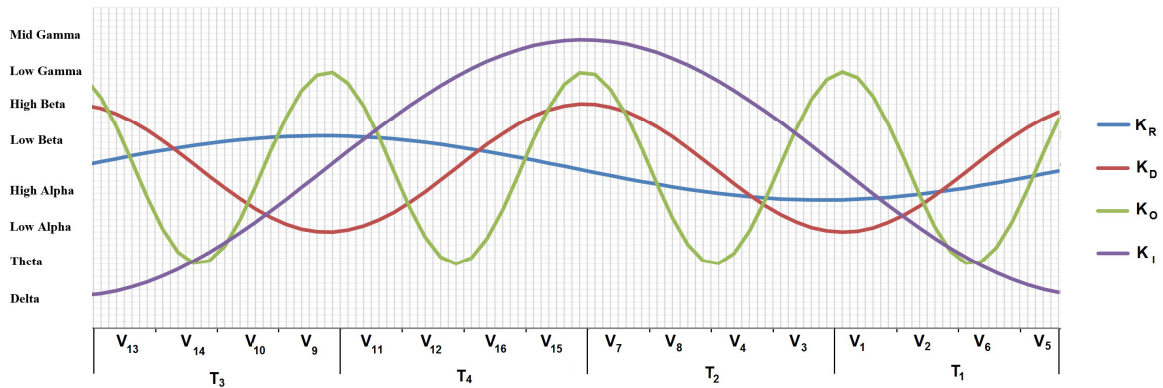


Figure 27: The diagram of behavioural functions in cognitive classes and the brain frequency bands.

#### 6.4 Variables, working procedure

The test was conducted in two steps of simultaneous EEG-EDA acquisition, i.e. at T1 and T2, with a break of 6 months between the steps.

During the experiment, the following were monitored in the EDA electrodermal activity:

-independent variables: the cognitive functions: Ia, Ib, Oa, Ob, Da, Db, Ra, Rb and the behavioural functions type  $K_i$  (I\_EDA, O\_EDA, D\_EDA, R\_EDA) and the probabilities and shares thereof, determined in the process of identifying the cognitive typology;

-dependant variables: the level of basal (SPL) and response (SPR) electrodermal potential;

The following were monitored in the EEG activity:

-independent variables: the cognitive functions:  $F_1, F_2, F_3, F_4, F_5, F_6, F_7$  și  $F_8$  and the behavioural functions type  $K_i$  (I\_EEG, O\_EEG, D\_EEG, R\_EEG) and the probabilities and shares thereof, determined in the process of identifying the cognitive typology;

-dependant variables: the average of the spectral power densities in the Delta, Theta, Low Alpha, High Alpha, Low Beta, High Beta, Low Gamma, Mid Gamma bands.

In order to make a measurement, we achieved the measurement loop by positioning the Neuro Sky MindSet head piece on the subject's head and applying the subject's palms on the sensors of the palm scanner MindSpring™. We started the EEG head piece, the scanner and the acquisition

interfaces MindMi™ and Open VIBE v1.2.2. At the level of the software interface for mixed evaluation, we conducted the primary processing and listed the values for inferential functions, as also calculated the cognitive functions EEG and EDA.

The EDA biodata were acquired with a sampling rate of 20 readings/ second [Grigore, 2013] and the EEG biodata were acquired with a sampling rate of 512 readings/ second.

For numeric evaluation, the following measurement units were used:

- for potentials of electrodermal response – [mV];
- for inferential functions - conventional units [u.inf.]; for cognitive functions and behavioural functions - scale (25 - 265);
- for spectral power densities: accuracy units [aq.u.PDS], specific to the measurement instrument, on the scale (0 - 12).

The final correlation analysis of the data was made with PASW Statistics 20.

The experimental data are shown in Appendix 1.

In order to obtain the correspondence between the two types of biosignals, reflected in the personality typology, we used two ways: analysis of the correspondence of the shares of cognitive typologies, as described in 5.1.3, and correlation analysis of the probabilities of the cognitive functions, as described in 5.1.4.

For the correlation analysis, we used the Pearson coefficient as statistic tool, by means of which the level of the correlation between variables was tested. The correlation was tested progressively, as follows:

1. The correlation of the total sums of the probabilities of the cognitive functions at  $T_1$  and  $T_2$ ;
2. The correlation of the sums of the probabilities of the cognitive functions VHI-VLO at  $T_1$  and  $T_2$ ;
3. The correlation of the sums of the probabilities of the cognitive functions HI-LO at  $T_1$  and  $T_2$ ;
4. The correlation of the probabilities of the *tonic* and *atonic* cognitive functions at  $T_1$  and  $T_2$ ;

Also, using the relations (48), (49), (50), (51) și (52) we evaluated the shares of the cognitive typologies at  $T_1$  and  $T_2$ .

### 6.5 The Pearson bivariate correlation analysis

*Pearson coefficient* used in this research reveals the correlation between two continuous variables, being also referred to as the product-moment or *Pearson r coefficient*. A positive value  $r$  expresses a positive relation between the two variables (A higher, B higher), while a negative value  $r$  indicates a negative relation (A lower, B lower). A correlation coefficient

equal to zero indicates no relation between the variables.

*The correlation of the total sums of the probabilities of the cognitive functions at  $T_1$  and  $T_2$ .*

As shown in 5.1.4, using the Kolmogorov's axioms, we calculated the probabilities of the cognitive functions that decide the behavioural functions according to (48), for the two sets of data taken from a sample of 100 subjects, at the moments  $T_1$  and  $T_2$ . The arrays of values resulting from the sum of all these functions, grouped based on their specific physiological category, were subject to the correlation analysis. Hence, Table 8 shows values of the Pearson coefficient that indicate a very good association between the values corresponding to the same type of biosignals  $T_1$  and  $T_2$ : 0.868 for EDA, 0.861 for EEG. This indicates a high test-retest reliability, for both types of biosignals.

A very good relation level was also obtained between the total sums for EDA-EEG, of 0.840 at  $T_1$  and 0.829 at  $T_2$ , value that indicate test-retest reliability between the two evaluation systems, this being a first confirmation of the working assumption.

*The correlation of the sums of the probabilities of the cognitive functions VHI-VLO at  $T_1$  and  $T_2$ .*

In the logic of the above results there are also included those presented in the Tables 9 and 10 concerning the systematization of the overall cognitive functions after brain frequency. Given that the determined probabilities for correlation analysis are subject to the relation (53), and in selecting the cognitive function we used (48), the results of the correlation level for antagonistic frequency categories will be symmetric against zero. We can find very good correlation values for the EDA-EEG functions of very high and very low frequency, of 0.884 at  $T_1$  and 0.838 at  $T_2$ . Also these values, as with the total sums of the probabilities of cognitive functions, confirm the high test-retest reliability of the two measurement systems and, by this, also confirms the working assumption.

*The correlation of the sums of the probabilities of the cognitive functions HI-LO at  $T_1$  and  $T_2$ .*

A third confirmation of the working assumption is brought by the values of the Pearson bivariate correlation coefficient, presented in the Tables 11 and 12 also in the EDA-EEG low and high-frequency functions, of 0.830 at  $T_1$  and 0.849 at  $T_2$ .

*The correlation of the probabilities of the tonic and atonic cognitive functions at  $T_1$  and  $T_2$ .*

The determination of the cognitive functions in their individual form, but sorted based on the criteria presented in 5.1.3 and 6.3, represent the most important part of this experimental work. Subject to the same methods for identification of probabilities they are found with, from one measurement step ( $T_1$ ) to another ( $T_2$ ), in the selection structure of the cognitive typologies (48), the values of the cognitive

functions presented in the Tables 13, 14, 15 and 16 also correlate, confirming the working assumption. Very high values have been obtained: 0.980 for Ia-F<sub>1</sub> (and the symmetric pair Ib-F<sub>2</sub>) and 0.948 for Ra-F<sub>7</sub> (and Rb-F<sub>8</sub>) at T<sub>1</sub>, and 0.920 for Ia-F<sub>1</sub> (and the symmetric pair Ib-F<sub>2</sub>) and 0.948 for Ra-F<sub>7</sub> (and Rb-F<sub>8</sub>) at T<sub>2</sub>. Values that reflect a very good moderate correlation were obtained on the pairs: Oa-F<sub>3</sub> (Ob-F<sub>4</sub>), 0.689 at T<sub>1</sub> and 0.629 at T<sub>2</sub>, and 0.675 for Da-F<sub>5</sub> (Db-F<sub>6</sub>) and 0,777 for Da-F<sub>5</sub>(Db-F<sub>6</sub>) at T<sub>2</sub>, an explanation for these slightly low values from the first being the specific of the way of integrating the dependant values and the biosignals. The MindSet head piece from NeuroSky shows, for EEG signals, an overlap of a number of simple signals with amplitude usually varying from about 1V at 100 V for a normal adult and about 10 - 20 mV, if measured with subdural electrodes, such as the FFT electrodes. The *phasic neurostimulator* measures response electrical signals of which values can be followed between 18 and 435 mV, depending on the internal structure of the stimulation equipment. In this latter case, the signal integration is global, the signal being expressed in the response in the SPR potentials obtained by phasic stimulation and projectively deducted in values of the *inferential functions*.

### 6.6 Shares correspondence analysis

A very precise form of identification of the readability of a cognitive typology in mixed EEG-EDA determinations was achieved with the method described in 5.1.3.

Table 17 shows the percentage result of the shares of EDA and EEG cognitive typologies found in T1 and T2, thus, in the same category of biosignals we determined a share of 92.25% for EEG and 92% for EDA and for mixed category, 91.75% at T1 and 91.5 at T2. Table 18 also shows the correspondence of the shares of the behavioural functions at T1 and T2, where the values corresponding to the function I, deducted from Ia and Ib (F1 and F2) are 99% at T1 and 96% at T2, the values corresponding to the function O, deducted from Oa and Ob (F3 and F4) are 84% at T1 and 81% at T2. The function D deducted from Da and Db (F5 and F6) shows 86% at T1 and 91% at T2 and the R function deducted from Ra and Rb (F7 and F8) shows the same value of 98% at T1 and T2.

The correspondences of the shares of *cognitive functions* presented in Table 19 are also reflected by high values: 91.59% at T1, for very high and very low frequency bands, 92% at T1 for high and low frequencies, and 88.59% at T1 for very high and very low frequency bands, 94.59% at T1 for high and low frequencies, values that also confirm the working assumption.

## 6.7 Experimental results

Table 8. The correlation of the total sums of the probabilities of the cognitive functions at T<sub>1</sub> and T<sub>2</sub>

|                               | P(EDA_T1) | P(EDA_T2) | P(EEG_T1) | P(EEG_T2) |
|-------------------------------|-----------|-----------|-----------|-----------|
| P(EDA_T1) Pearson Correlation | 1         | .868**    | .840**    | .757**    |
| Sig. (2-tailed)               |           | .000      | .000      | .000      |
| N                             | 100       | 100       | 100       | 100       |
| P(EDA_T2) Pearson Correlation | .868**    | 1         | .748**    | .829**    |
| Sig. (2-tailed)               | .000      |           | .000      | .000      |
| N                             | 100       | 100       | 100       | 100       |
| P(EEG_T1) Pearson Correlation | .840**    | .748**    | 1         | .861**    |
| Sig. (2-tailed)               | .000      | .000      |           | .000      |
| N                             | 100       | 100       | 100       | 100       |
| P(EEG_T2) Pearson Correlation | .757**    | .829**    | .861**    | 1         |
| Sig. (2-tailed)               | .000      | .000      | .000      |           |
| N                             | 100       | 100       | 100       | 100       |

Table 9. The correlation of the sums of the probabilities of the cognitive functions VHI-VLO at T<sub>1</sub>

|                                   | P(VHI_EEG_T1) | P(VLO_EEG_T1) |
|-----------------------------------|---------------|---------------|
| P(VHI_EDA_T1) Pearson Correlation | .884**        | -.884**       |
| Sig. (2-tailed)                   | .000          | .000          |
| N                                 | 100           | 100           |
| P(VLO_EDA_T1) Pearson Correlation | -.884**       | .884**        |
| Sig. (2-tailed)                   | .000          | .000          |
| N                                 | 100           | 100           |

Table 10. The correlation of the sums of the probabilities of the cognitive functions VHI-VLO at T<sub>2</sub>

|                                   | P(VHI_EEG_T2) | P(VLO_EEG_T2) |
|-----------------------------------|---------------|---------------|
| P(VHI_EDA_T2) Pearson Correlation | .838**        | -.838**       |
| Sig. (2-tailed)                   | .000          | .000          |
| N                                 | 100           | 100           |
| P(VLO_EDA_T2) Pearson Correlation | -.838**       | .838**        |
| Sig. (2-tailed)                   | .000          | .000          |
| N                                 | 100           | 100           |

Table 11. The correlation of the sums of the probabilities of the cognitive functions HI-LO at T<sub>1</sub>

|                                  | P(HI_EEG_T1) | P(LO_EEG_T1) |
|----------------------------------|--------------|--------------|
| P(HI_EDA_T1) Pearson Correlation | .830**       | -.830**      |
| Sig. (2-tailed)                  | .000         | .000         |
| N                                | 100          | 100          |
| P(LO_EDA_T1) Pearson Correlation | -.830**      | .830**       |
| Sig. (2-tailed)                  | .000         | .000         |
| N                                | 100          | 100          |

Table 12. The correlation of the sums of the probabilities of the cognitive functions HI-LO at T<sub>2</sub>

|              |                     | P(HI_EEG_T2) | P(LO_EEG_T2) |
|--------------|---------------------|--------------|--------------|
| P(HI_EDA_T2) | Pearson Correlation | .849**       | -.849**      |
|              | Sig. (2-tailed)     | .000         | .000         |
|              | N                   | 100          | 100          |
| P(LO_EDA_T2) | Pearson Correlation | -.849**      | .849**       |
|              | Sig. (2-tailed)     | .000         | .000         |
|              | N                   | 100          | 100          |

Table 13. The correlation of the probabilities of the tonic cognitive functions at T<sub>1</sub>

|          |                     | P(la_T1) | P(Oa_T1) | P(Da_T1) | P(Ra_T1) |
|----------|---------------------|----------|----------|----------|----------|
| P(F1_T1) | Pearson Correlation | .980**   | .673**   | .291**   | -.363**  |
|          | Sig. (2-tailed)     | .000     | .000     | .003     | .000     |
|          | N                   | 100      | 100      | 100      | 100      |
| P(F3_T1) | Pearson Correlation | .376**   | .689**   | .062     | -.315**  |
|          | Sig. (2-tailed)     | .000     | .000     | .540     | .001     |
|          | N                   | 100      | 100      | 100      | 100      |
| P(F5_T1) | Pearson Correlation | .262**   | .260**   | .675**   | .067     |
|          | Sig. (2-tailed)     | .008     | .009     | .000     | .506     |
|          | N                   | 100      | 100      | 100      | 100      |
| P(F7_T1) | Pearson Correlation | -.373**  | -.490**  | .052     | .948**   |
|          | Sig. (2-tailed)     | .000     | .000     | .606     | .000     |
|          | N                   | 100      | 100      | 100      | 100      |

Table 14. The correlation of the probabilities of the tonic cognitive functions at T<sub>2</sub>

|          |                     | P(la_T2) | P(Oa_T2) | P(Da_T2) | P(Ra_T2) |
|----------|---------------------|----------|----------|----------|----------|
| P(F1_T2) | Pearson Correlation | .920**   | .632**   | .146     | -.281**  |
|          | Sig. (2-tailed)     | .000     | .000     | .147     | .005     |
|          | N                   | 100      | 100      | 100      | 100      |
| P(F3_T2) | Pearson Correlation | .451**   | .629**   | .063     | -.289**  |
|          | Sig. (2-tailed)     | .000     | .000     | .536     | .004     |
|          | N                   | 100      | 100      | 100      | 100      |
| P(F5_T2) | Pearson Correlation | .251*    | .105     | .777**   | .113     |
|          | Sig. (2-tailed)     | .012     | .299     | .000     | .264     |
|          | N                   | 100      | 100      | 100      | 100      |
| P(F7_T2) | Pearson Correlation | -.334**  | -.375**  | .014     | .948**   |
|          | Sig. (2-tailed)     | .001     | .000     | .888     | .000     |
|          | N                   | 100      | 100      | 100      | 100      |

Table 15. The correlation of the probabilities of the atonic cognitive functions at T<sub>1</sub>

|          |                     | P(F2_T1) | P(F4_T1) | P(F6_T1) | P(F8_T1) |
|----------|---------------------|----------|----------|----------|----------|
| P(lb_T1) | Pearson Correlation | .980**   | .376**   | .262**   | -.373**  |
|          | Sig. (2-tailed)     | .000     | .000     | .008     | .000     |
|          | N                   | 100      | 100      | 100      | 100      |
| P(Ob_T1) | Pearson Correlation | .673**   | .689**   | .260**   | -.490**  |
|          | Sig. (2-tailed)     | .000     | .000     | .009     | .000     |
|          | N                   | 100      | 100      | 100      | 100      |
| P(Db_T1) | Pearson Correlation | .291**   | .062     | .675**   | .052     |
|          | Sig. (2-tailed)     | .003     | .540     | .000     | .606     |
|          | N                   | 100      | 100      | 100      | 100      |
| P(Rb_T1) | Pearson Correlation | -.363**  | -.315**  | .067     | .948**   |
|          | Sig. (2-tailed)     | .000     | .001     | .506     | .000     |
|          | N                   | 100      | 100      | 100      | 100      |

Table 16. The correlation of the probabilities of the atonic cognitive functions at T<sub>2</sub>

|          |                     | P(F2_T2) | P(F4_T2) | P(F6_T2) | P(F8_T2) |
|----------|---------------------|----------|----------|----------|----------|
| P(lb_T2) | Pearson Correlation | .920**   | .451**   | .251*    | -.334**  |
|          | Sig. (2-tailed)     | .000     | .000     | .012     | .001     |
|          | N                   | 100      | 100      | 100      | 100      |
| P(Ob_T2) | Pearson Correlation | .632**   | .629**   | .105     | -.375**  |
|          | Sig. (2-tailed)     | .000     | .000     | .299     | .000     |
|          | N                   | 100      | 100      | 100      | 100      |
| P(Db_T2) | Pearson Correlation | .146     | .063     | .777**   | .014     |
|          | Sig. (2-tailed)     | .147     | .536     | .000     | .888     |
|          | N                   | 100      | 100      | 100      | 100      |
| P(Rb_T2) | Pearson Correlation | -.281**  | -.289**  | .113     | .948**   |
|          | Sig. (2-tailed)     | .005     | .004     | .264     | .000     |
|          | N                   | 100      | 100      | 100      | 100      |

Notes:

\*\* . Correlation is significant at the 0.01 level (2-tailed).

\* . Correlation is significant at the 0.05 level (2-tailed).

Table 17. The correspondence of the shares of cognitive typologies at T<sub>1</sub> and T<sub>2</sub>.

|        |        |        |
|--------|--------|--------|
| EEG_T1 | 91,75% | EDA_T1 |
| 92,25% |        | 92%    |
| EEG_T2 | 91,5%  | EDA_T2 |

Table 18. The correspondence of the shares of *behavioural typologies* at T<sub>1</sub> and T<sub>2</sub>.

|    |     |   |     |    |
|----|-----|---|-----|----|
| T1 | 99% | I | 96% | T2 |
|    | 84% | O | 81% |    |
|    | 86% | D | 91% |    |
|    | 98% | R | 98% |    |

Table 19. The correspondence of the shares of *cognitive typologies* at T<sub>1</sub> and T<sub>2</sub>.

|                   |        |                   |
|-------------------|--------|-------------------|
| EEG_T1<br>VHI;VLO | 91,59% | EDA_T1<br>VHI;VLO |
| EEG_T1<br>HI;LO   | 92%    | EDA_T1<br>HI;LO   |
| EEG_T2<br>VHI;VLO | 88,59% | EDA_T2<br>VHI;VLO |
| EEG_T2<br>HI;LO   | 94,59% | EDA_T2<br>HI;LO   |

## 6.8 Conclusions

The comparative experiment described in this work confirms the working assumption, i.e. there is a significant correlation between the values of the *cognitive functions* determined from the average of the *spectral power densities* of the EEG biosignals taken from the scalp level and the *cognitive functions* corresponding to the basal (SPL) and response (SPR) electrodermal potential measured at the same time, at the palms of the same individual, through the *phasic neurostimulation method*, and the design used reflects simultaneous and joint

action of the targeted functions in the process of determining a psychological profile through the two types of biosignals. There are also provided the assumptions based on which a future study may be conducted on the correspondences between the palm areas and the locations of the EEG sensors in the "10-20 American System".

The study also reveals that there is a functional difference between the EEG signals, which we consider predominantly *signals of interest in functional explorations (neurophysiology)*, them being connected to subsystems having a strictly specialised brain activity, and the EDA signals - stimulated, which are *signals of general interest in psychology and psychopathology*, them being capable of correlation with the subsystems with integrated mental activity.

This research brings highly valuable experimental arguments in connection with the possibility for the psychometric system MindMi™ used here for the determinations of electrodermal response to evaluate some psychophysiological aspects, at least to the same extent as the systems from the class of equipment based on electroencephalogram-type signals, significantly maintaining, through the manner of integrating the brain signals, projectively determined, on time units much wider than the potentials evoked in the EEG, the specificity to be useful particularly in psychological assessments. This nevertheless does not limit its possibilities of use in clinical assessments, where it can bring additional definition in establishing a diagnosis.

## Reference

- [Ashrafulla, 2001] Ashrafulla, S.: "EEG and MEG : functional brain imaging with high temporal resolution" in "Electrical signals in the brain", 2001, Legătură accesată la 9 august 2015: [https://ngp.usc.edu/files/2013/06/Syed\\_EEG\\_MEG.pdf](https://ngp.usc.edu/files/2013/06/Syed_EEG_MEG.pdf)
- [Baker, 1989] Baker, L.E. „Principles of the impedance technique”. IEEE Eng. Med. Biol. Mag. 3:11–15, 1989
- [Barnett & Bagno, 1936] Barnett, A., & S. Bagno. „The physiological mechanisms involved in the clinical measure of phase angle”. Am. J. Physiol. 114:366–382, 1936
- [Baumgartner, Chumlea & Roche, 1988] Baumgartner, R.N., W.C. Chumlea, and A.F. Roche, Bioelectric impedance phase angle and body composition. Am. J. Clin. Nutr. 48:16–23, 1988
- [Bloch, Roland, Eric & Alain, 2006] Bloch, H., Roland, C., Eric, D., & Alain, G. Larousse - Marele dicționar al psihologiei. București, Editura Trei, 407, 2006
- [Boucsein, 2012] Boucsein, W., *Electrodermal Activity*, Second edition, © Springer Science + Business Media, LLC, 2012
- [Boucsein, Schaeffer & Neijenhuisen, 1989] Boucsein, W., Schaefer, F., Neijenhuisen, H. (1989). "Continuous recordings of impedance and phase angle during electrodermal reactions and the locus of impedance change". *Psychophysiology*, 26(3), 369-76, 1989
- [Burger, 2014] Burger, C., "A novel method of improving EEG signals for BCI classifications", Stellenbosch University, South Africa, 2014
- [Cacioppo & Tassinari, 1990] Cacioppo, J.T., & Tassinari, L.G., "Inferring Psychological Significance from Physiological Signals", *American Psychological Association*, 45(I), 16-28, 1990

10. [Christie, 1981] Christie, M.J., "Electrodermal activity in the 1980s: a review", Journal of the Royal Society of Medicine Volume 74, August 1981
11. [Chumlea & Guo, 1997] Chumlea, W. C., & Guo, S. S. „Bioelectrical impedance: a history, research issues, and recent consensus”. In: „Emerging Technologies for Nutrition Research”, edited by S. J. Carlson-Newberry and R. B. Costello. Washington, DC: Natl. Acad. Press, 169–192, 1997
12. [Dornhege, Millán, Hinterberger, McFarland, Müller & Sejnowski, 2007] Dornhege, G.; Millán, J. del R.; Hinterberger, T.; McFarland, D. J.; Müller, K-R; Sejnowski, T. J. "An introduction to brain computer interfacing". In: Towards Brain-Computer Interfacing, MIT Press, Cambridge, 2007
13. [Edelberg, 1968] Edelberg R., "Biopotentials from the skin surface: The hydration effect", "Annals of the New York Academy of Sciences", *Bioelectrodes*, 148, 252–262, February 1968;
14. [Fisslinger, 1998] Fisslinger, R.J., (1998), "Interactive computer assisted multi-media biofeedback system", United States Patent, US3841316, 1998
15. [Forslund, 2003] Forslund, P.: "A Neural Network Based Brain - Computer Interface for Classification of Movement Related EEG"., Linköping University, December, 2003
16. [Fox, 2009] Fox, S.I.: "Fundamentals of Human Physiology", McGraw-Hill, New York, 2009
17. [Fowles, 1986] Fowles, DC, „The eccrine system and electrodermal activity” In *Psychophysiology*, ed. MGH Coles, E Donchin, SW Porges, pp. 51-96, Guilford Press, New York, 1986
18. [Fowles, Christie, Edelberg, Grings, Lykken & Venables, 1981]. Fowles, D.C., Christie, M. J., Edelberg, R., Grings, W. W., Lykken, D. T., & Venables, P. H. „Publication recommendations for electrodermal measurements”. *Psychophysiology*, 18, 232–239., 1981
19. [Gildemeister and Kaufhold, 1920] Gildemeister, M. and Kaufhold, R. (1920). Über das elektrische Leitungsvermögen der über-tetenden menschlichen Haut. *Pflügers Arch. f. d. ges. Physiol.*, 179: 154, 1920.
20. [Grigore, 2013] Grigore, D., „Echipament electronic și metodă pentru determinarea rapidă a profilului psihologic”, RO127615, OSIM, România 2013
21. [Grigore, 2014] Grigore, D., „Sistem psihometric integrat pentru evaluare complementară”, Editura ARGES PRESS, Pitești, ISBN 978-606-8506-11-1, 2014
22. [Grigore, R1, 2014] Grigore, D., „Tipuri de biosemnale electrice și aplicații în domeniul sistemelor tehnice - Raport de Cercetare Numărul 1”, Școala Doctorală, Academia Tehnică Militară, București, Octombrie, 2014
23. [Grigore, R2, 2015] Grigore, D., „Procesarea biosemnalelor și corelarea dintre biosemnal și controlul mișcării la distanță - Raport de Cercetare Numărul 2”, Școala Doctorală, Academia Tehnică Militară, București, Mai, 2015
24. [Grigore & Moldovan, 2015] Grigore, D., „MindMi™ Sistem de evaluare psihologică”, [www.psychometricsystems.com](http://www.psychometricsystems.com), 2015
25. [Grigore & Petrescu, 2015] Grigore, D., Petrescu, C., „Multiple correlations between EEG and GSR patterns on remote movement command and control”, "International Conference Greener and Safer Energetic and Ballistic Systems, GSEBS 2015", held at the Military Technical Academy Bucharest, ROMANIA, May 22nd – 23rd, 2015
26. [Grigore & Costache, 2015] Grigore D., Costache, G. C., „Comparative study regarding GSR and EEG type biosignals simultaneously answer to same external stimulus”, The International Conference „Education and Creativity for a Knowledge based Society – Psychology”, November 19nd-21rd, 2015, "Titu Maiorescu" University, pp. 103-108, Social Science Research Network (SSRN), ISSN 2248-003X, ISBN 978-3-9503145-6-4
27. [Grigore, R3, 2015] Grigore, D., „Studiu statistic privind prelucrarea datelor experimentale ale interacțiunii dintre biosemnale și controlul mișcării la distanță - Raport de Cercetare Numărul 3”, Școala Doctorală, Academia Tehnică Militară, București, Noiembrie, 2015
28. [Grigore, Paraschiv & Anghelina, 2016] Grigore, D., Paraschiv, R. V., Anghelina, L. O., „The action of multiple stimulations on GSR involved în remote movement command and control”, "International Conference Greener and Safer Energetic and Ballistic Systems, GSEBS 2016", held at the Military Technical Academy Bucharest, ROMANIA, May 26nd – 27rd, 2016
29. [Grigore, 2016] Grigore, D., „Metodă fractală inferențială”, "Sesiunea Științifică a Academiei Oamenilor de Știință din România", Durău, 22-24 septembrie, 2016
30. [Griessbach, Kudryevtseva, Henning, Harnampieva, Ivanova & Kirlengic, 2007]

- Griessbach G., Kudryevtseva, S. Henning., G. Harampieva, I., Ivanova, G., Kirlengic, E., M., "Method and device for detecting neurological and psycho-physiological states", Australian Patent Office, AU2006252068A1, 2007
31. [Hariton, 2009] Hariton, C., "Electronică medicală", UMF Iași, 2009
  32. [Hoffmann, Vesin, Ebrahimi & Diserens, 2008] Hoffmann, U.; Vesin, J.-M.; Ebrahimi, T. & Diserens K., "An efficient P300-based braincomputer interface for disabled subjects", Journal of Neuroscience Methods, 167(1), 115-125, 2008
  33. [INRIA, 2015] "OpenVibe - Software for Brain Computer Interface", Institut National de Recherche en Informatique et en Automatique, France, Legătură accesată la 15 aprilie 2015: <http://openvibe.inria.fr/downloads/>
  34. [Ivorra & Aguiló, 2001]. Ivorra, A., & Aguiló, J. „New five-electrode method for impedance measurement”. (176) 263-266 in International Conference on Electrical Bio-Impedance XI, Oslo, Norway, 2001
  35. [Ivorra & Rubinsky, 2007] Ivorra, A., & Rubinsky, B. (2007). „In vivo electrical impedance measurements during and after electroporation of rat liver”, Bioelectrochemistry 70 (2), 287-295, 2007
  36. [Kandel, Schwartz & Jessell, 1991] Kandel, E.R., Schwartz, J.H, Jessell, T.M., "Principles of Neural Science", 3rd Edition, London, Prentice Hall, 1991
  37. [Kay, Bothwell, & Foltz, 1954] Kay C.F., P.T. Bothwell, & E.L. Foltz (1954). „Electrical resistivity of living body tissues at low frequencies". J. Physiol. 13:131–136, 1954
  38. [Keirn & Aunon, 1990] Keirn, Z.A. & Aunon, J. "A new mode of communication between man and his surroundings". IEEE Transactions Biomedical Engineering, 37, 1209-1214, 1990
  39. [Korenman, 2000] Korenman, E.M.D., "Apparatus for monitoring a person's psycho-physiological condition", United States Patent, US6067468, 2000
  40. [Lawler, Davis & Griffith, 1960] Lawler, J.C., Davis, M.J., Griffith, E.C., „Electrical characteristics of the skin. The impedance of the surface sheath and deep tissues". J Invest Dermatol., 34:301-8, 1960
  41. [Libenson, 2012] Libenson, M.H.: "Practical Approach to Electroencephalography", 2012. ISBN 9781455745944.
  42. [Lopes, 2004] Lopes da Silva, F., "Functional localization of brain sources using EEG and/or MEG data: volume conductor and source models", Journal Magnetic Resonance Imaging, 22(10), 2004
  43. [Lopes, Hoeks, Smits & Zetterberg, 1974] Lopes da Silva, F. H., Hoeks, A., Smits, H., and Zetterberg, L. H., 'Model of brain rhythmic activity: the alpha-rhythm of the thalamus', *Kybernetik*, **15**, 1974, 27–37.
  44. [Lukaski & Bolonchuk, 1987]. Lukaski, H.C., & Bolonchuk, W.W. „Theory and validation of the tetrapolar bioelectrical impedance method to assess human body composition". in In Vivo Body Composition Studies, Ellis, J.K., Yasumura, S, & Morgan, W.D. eds. London: The Institute of Physical Sciences in Medicine, 49–60, 1987
  45. [Mayer, 1974] Mayer, R.W., "Apparatus for measuring the psychogalvanic reflex", United States Patent, US3841316, 1974
  46. [McFarland & Wolpaw, 2005] McFarland, D. J. & Wolpaw, J. R., "Sensorimotor rhythm-based brain-computer interface (BCI): feature selection by regression improves performance", "IEEE Transaction on Rehabilitation Engineering", 13(3), 372-379, 2005
  47. [McFarland et. al., 2005] McFarland, D.J., Sarnacki, W.A., Vaughan, T.M. and Wolpaw, J.R.: "Brain Computer interface (BCI) operation: Signal and noise during early training sessions", *Clinical Neurophysiology*, 116, 56–62, 2005. ISSN 13882457.
  48. [Menon & Crottaz-Herbette, 2005] Menon, V. and Crottaz-Herbette, S.: "Combined EEG and fMRI studies of human", *International Review of Neurobiology*, Elsevier Inc., 66(05), DOI: 10.1016/S0074-7742(05)66010-2, 2005.
  49. [NSKY, 2011] "Mind Wave - user guide" NEUROSKY.COM, Legătură accesată la 10 martie 2013: <https://www.neurosky.com/>
  50. [Nyboer, 1959] Nyboer, J. „Electrical Impedance Plethysmography". Springfield, Ill.: Charles C Thomas, 1959
  51. [Núñez & Srinivasan, 2009] Núñez, P.L. and Srinivasan, R.: "Electric Fields of the Brain: The neurophysics of EEG" An Overview of Electromagnetic Fields, C, 1–2, 2009
  52. [Papoulis, 1977] "Signal Analysis". New York: McGraw-Hill, 1977
  53. [Paraschiv, Grigore & Constantin, 2013] Paraschiv T., Grigore D., Constantin A., "Modelarea neurosemnalelor electrodermice stimulate fazic", Conferința Națională „SISTEME ENERGETICE ȘI BALISTICE – SEB 2013", Academia Tehnică Militară, București, 19-20 septembrie, 2013;
  54. [Paraschiv, Postolea, Ionescu & Grigore, 2014] Paraschiv, T.; Postolea, D., Ionescu, D., Grigore, D., "Metodă de procesare a

- semnalelor EEG*", The International Conference "Education and Creativity for a Knowledge based Society-Psychology", "Titu Maiorescu" University, Bucharest, June 21nd-23rd, 2014, ISSN 2248-0064;
55. [Paraschiv, Grigore & Ștefan, 2015] Paraschiv T., Grigore D., Ștefan C., "The mathematics processing of signals", "International Conference Greener and Safer Energetic and Ballistic Systems, GSEBS 2015", held at the Military Technical Academy Bucharest, ROMANIA, May 22nd – 23rd, 2015;
  56. [PEERJ, 2016] "Consumer-grade EEG devices: are they usable for control tasks?", *PeerJ*, Legătură accesată la 24 iulie 2016: <https://peerj.com/articles/1746.pdf>
  57. [Porat, 1994] Digital Processing of Random Signals — Theory and Methods. Englewood Cliffs, NJ: Prentice Hall, 1994
  58. [Postolea, Ștefan & Grigore, 2013] Postolea D., Ștefan C., Grigore D., "Controlul mișcării utilizând investigarea biosemnalelor de tip EEG", Conferința Națională „SISTEME ENERGETICE ȘI BALISTICE – SEB 2013”, Academia Tehnică Militară, București, 19-20 septembrie, 2013;
  59. [Sanei & Chambers, 2008] Sanei, S. and Chambers, J.: EEG signal processing. 2008. ISBN 9780470025819. Legătură accesată la 9 august 2015: <http://medcontent.metapress.com/index/A65RM03P4874243N.pdf><http://books.google.com/>
  60. [Schwartz & Andrasik, 2003] Schwartz M.S., Andrasik, F., "Biofeedback", Third Edition: A Practitioner's Guide, The Guilford Press, New York, 2003
  61. [Schwan & Kay, 1956] C.F. Schwan, H.P., & Kay, C.F. "The conductivity of living tissues". *Ann. N.Y. Acad. Sci.* 65:1007-1013, 1956
  62. [Stoica & Moses, 2005] Stoica, P., Moses, R., "Spectral Analysis of Signals" PRENTICE HALL, Upper Saddle River, New Jersey 07458, 2005
  63. [Subramanyan, Manchanda, Nyboer & Bhatia, 1980] Subramanyan, R., Manchanda, S.C., Nyboer, J., & Bhatia, M.L. "Total body water in congestive heart failure. A pre-and post-treatment study". *J. Assoc. Physicians India*, 28, 257–262., 1980
  64. [Sălceanu, Iacobescu & Anghel, 2013] Sălceanu, A., Iacobescu, F., Anghel, M. "Upon the Influence of the Real Value of Human Body Capacitance in ESD Immunity Tests". *Proc. of 19th IMEKO TC 4 Symp.*, Barcelona, Spain, 501-507.
  65. [Sutherland, Dorr & Gomatom, 2005] Sutherland, P.E., Dorr, D., Gomatom, K., Human Current Sensitivities and Resistance Values in the Presence of Electrically Energized Objects. *IEEE Ind. a. Comm. Power Syst. Techn. Conf.*, 159-167., 2005
  66. [Teplan, 2002] Teplan, M.: "Fundamentals of EEG measurement", *Measurement Science Review*, 2, 1–11, 2002.
  67. [Turpin & Clements, 1993] Turpin, G., Clements, K., "Electrodermal activity and psychopathology; the development of the palmar sweat index (PSI) as an applied measure for use in clinical settings; *Progress in Electrodermal Research*", Edited by J.-C. Roy et al. Plenum Press, New York, 1993
  68. [Wang, 1964] Wang, G. H., "The neural control of sweating", University of Wisconsin Press, 1964
  69. [Wilson & Cowan, 1972] Wilson, H. R., and Cowan, J. D., 'Excitatory and inhibitory interaction in localized populations of model neurons', *J. Biophys.*, 12, 1972, 1–23.
  70. [Wolpaw, Birbaumer, McFarland, Pfurtscheller & Vaughan, 2002] Wolpaw, J.R., Birbaumer, N., McFarland, D.J., Pfurtscheller, G. and Vaughan, T.M.: "Brain-computer interfaces for communication and control". *Clinical neurophysiology: official journal of the International Federation of Clinical Neurophysiology*, 113(6), 767–91, June 2002. ISSN 1388-2457. Legătură accesată la 9 august 2015: <http://www.ncbi.nlm.nih.gov/pubmed/12048038>
  71. [Zetterberg, 1973] Zetterberg, L. H., 'Stochastic activity in a population of neurons—a system analysis approach', Report of the Institute of Medical Physics, TNO, Utrecht, Vol. 1, 1973, 53.
  72. [Zinke-Allmang, 2009] Zinke-Allmang, M.: "Physics for the Life Sciences". 1st edn. Nelson, Toronto, 2009